UC San Diego

UC San Diego Electronic Theses and Dissertations

Title

The Effect of Shear Stress Patterns on Histone 3 Modification of Endothelial Cells

Permalink

https://escholarship.org/uc/item/76n1j9gb

Author

Leong, Samantha Antonio

Publication Date

2020

Peer reviewed|Thesis/dissertation

UNIVERSITY OF CALIFORNIA SAN DIEGO

The Effect of Shear Stress Patterns on Histone 3 Modification of Endothelial Cells

A Thesis submitted in partial satisfaction of the requirements

for the degree Master of Science

in

Bioengineering

by

Samantha Antonio Leong

Committee in charge:

Professor Shu Chien, Chair

Professor Shankar Subramaniam

Professor Sheng Zhong

2020

The Thesis of Samantha Antonio Leong is approved, and it is acceptable in quality and form for publication on microfilm and electronically:

_____

_____

_____

Chair

University of California San Diego

2020

Dedication

I would like to thank Dr. Shu Chien for providing me with this incredible opportunity, as well as Dr. Julie Yi-shuan Li and Dr. Li-jing Chen for providing me with unlimited support and guidance during every step of my journey. I am also indebted to the patience of Phu Nguyen and Jerry Norwich, from whom I have learned so much. Despite the trying times during lockdown, this thesis could not have been written without the support of every single person in the Chien Lab.

I am very grateful to my parents for all their sacrifices and for being my pillars of strength. Finally, my deepest gratitude to my biggest champion and sister, Amanda, without whom I would not be the person I am today.

Table of Contents

List of Figures

List of Tables

Abstract of the Thesis

The Effect of Shear Stress Patterns on Histone 3 Modification of Endothelial Cells

by

Samantha Antonio Leong

Master of Science in Bioengineering

University of California San Diego, 2020

Professor Shu Chien, Chair

Endothelial cells covering the inner surface of blood vessels are constantly exposed to shear stresses. Such hemodynamic shear stress influences vascular functions, and endothelial dysfunction can lead to the progression of cardiovascular diseases, such as atherosclerosis. Atherosclerotic plaque formation in the endothelium is shown to be site-specific: disturbed flow regions at lesser curvature of the aortic arch and branched points are sites that are more susceptible to plaque formation, whereas steady flow regions at greater curvature and straight parts are more atheroprotective and maintain vascular homeostasis. Previous

researches have extensively studied the various biochemical pathways implicated in atherosclerosis. Recently, increased attention has been granted to epigenetics to study the chromatin-based mechanisms in the nucleus involved in the regulation of gene expression in a DNA-independent manner. Studies have shown that histone modifications, such as methylation, are involved in different shear stress patterns. This thesis aims to compare the effects exerted by pulsatile shear (PS) and oscillatory shear (OS) on histone modifications, specifically H3K9 di- and tri- methylation (H3K9me3 and H3K9me3), in human umbilical vein endothelial cells (HUVECs) for 24 hours through chromatin immunoprecipitation followed by high throughput sequencing (ChIP-seq). Bioinformatics analysis of the flow-regulated H3K9me2/me3 enrichment genes using gene ontology (GO) analysis reveals pathways of mechnotransduction, inflammation, proliferation, migration, and apoptosis are involved in the atheroprotective effects of PS. Based on the identification of biological processes and functions in PS, such findings could be helpful in elucidating the various epigenetic elements involved in the development of atherosclerosis.

1 General Introduction to Hemodynamic Forces, Atherosclerosis, and Histone Modifications

1.1 Hemodynamic Forces, Endothelial Cells, and Atherosclerosis

Hemodynamic Forces Fluid shear stress is defined as the tangential component of frictional forces generated at a surface by the flow of a viscous fluid. In this case, fluid shear stress is generated by blood and acts on endothelial cells (ECs) that line the blood vessel [1]. Blood pressure causes the circumferential stretching normal to the vessel wall on both the ECs and the vascular smooth muscle cells (SMCs) that surround the endothelium in the arteries (Figure 1.1). Vascular physiology in adults is controlled by shear and pressure, amongst other factors.

Shear stress is expressed in Pascal (Pa) in the SI system (Système International). In the cardiovascular system, dyn/cm^2 is used instead, where $1\,Pa = 10\,dyn/cm^2$.
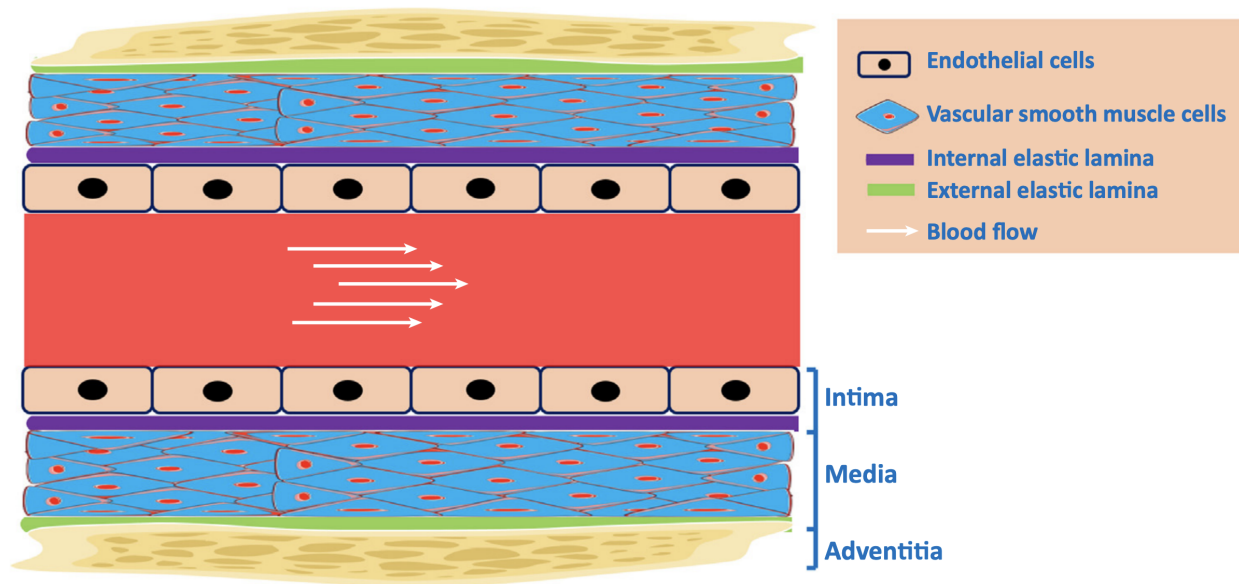
Figure 1.1: Vascular components of the artery.
Blood vessels are usually composed of three layers: the tunica intima, tunica media, and tunica adventitia. The intima consists of a monolayer of endothelial cells that line the vessel lumen. The endothelial cells are the major cell type that are constantly exposed to hemodynamic forces from blood flow. The tunica media is mainly composed of VSMCs. The tunica adventitia is primarily composed of connective tissues made up of fibroblasts, macrophages, and associated collagen-rich matrix proteins. [2]

Endothelial cells Blood vessels are continuously exposed to cyclic stretch and shear stress due to the pulsatile nature of blood pressure and flow. Shear stress is mainly borne by ECs, whereas SMCs are

mainly exposed to cyclic stretch from pulsatile pressure.

Vascular ECs form the inner lining of the blood vessel wall. Besides providing a selective barrier for macromolecular permeability, ECs are responsible for vascular remodelling through the production of growth-promoting and -inhibiting substances; modulate hemostasis/thrombosis through pro-coagulant, anti-coagulant, and fibrinolytic agents; mediate inflammatory responses through chemotactic and adhesion molecules expressed on membrane surface; regulate vascular SMC contraction through the vasodilators and vasoconstrictors [3]. Impairments in these functions may lead to conditions that develop into diseases such as atherosclerosis and/or thrombosis.

Among various stimuli that affect regulatory effects, mechanical factors from blood flow plays an important role of vascular physiology. Such hemodynamic forces determine vascular morphogenesis and physiology. Blood flow is essential to blood vessel development during development and regulation in diameter later in life. Flow induces dose dependent secretion of nitric oxide (NO) and prostacyclin, which relax smooth muscle and decrease vascular tone, a homeostatic mechanism that maintains constant fluid shear stress. While fluid shear stress within the physiological ranges stabilizes blood vessels, prolonged low or high flow causes inward or outward remodeling of the vessel wall respectively [4].

Mechanosensing and signaling in ECs in response to shear stress Application of shear stress to ECs leads to the activation of mechanosensors on the cell membrane. These sensors include integrins, tyrosine kinase receptors, G proteins and G-protein-coupled receptors, ion channels, and intercellular junction proteins. Some local membrane structures include caveolae, gap junctions, membrane lipids, and glycocalyx. Mechanosensing is transmitted through adaptor molecules and thus triggers a cascade of signalling pathways. Some of them include triggering signaling molecules like Ras, Rho, phosphatidylinositol-3-kinase (PI3K), and mitogen-activated protein kinases (MAPKs). They then activate endothelial nitric oxide synthase (eNOS), Smad1/4, and various transcription factors and cofactors, such as Kruppel-like factor 2 (KLF2), nuclear factor-κB (NF-κB), and activator protein 1 (AP-1) [5]. Such pathways then modulate the expression of functional genes (Figure 1.2). Some genes of interest can be grouped into categories, such as inflammation, oxidation, proliferation, migration, and cell cycle.

Atherosclerosis Atherosclerosis is a chronic inflammatory disease of arteries resulting from the interactions between modified lipoprotein, macrophages, T cells, and cellular elements in the arterial wall. These processes lead to the formation of lesions, or plaque, that protrudes into the lumen. The formation of plaque begins as fatty streaks that develop into intermediate lesions and slowly form fibrous and complex plaque. One of the most crucial cellular elements involved in atherosclerosis are the endothelial cells that line in inner arterial wall as a monolayer, known as the endothelium, as they are the interface where plaque may form.
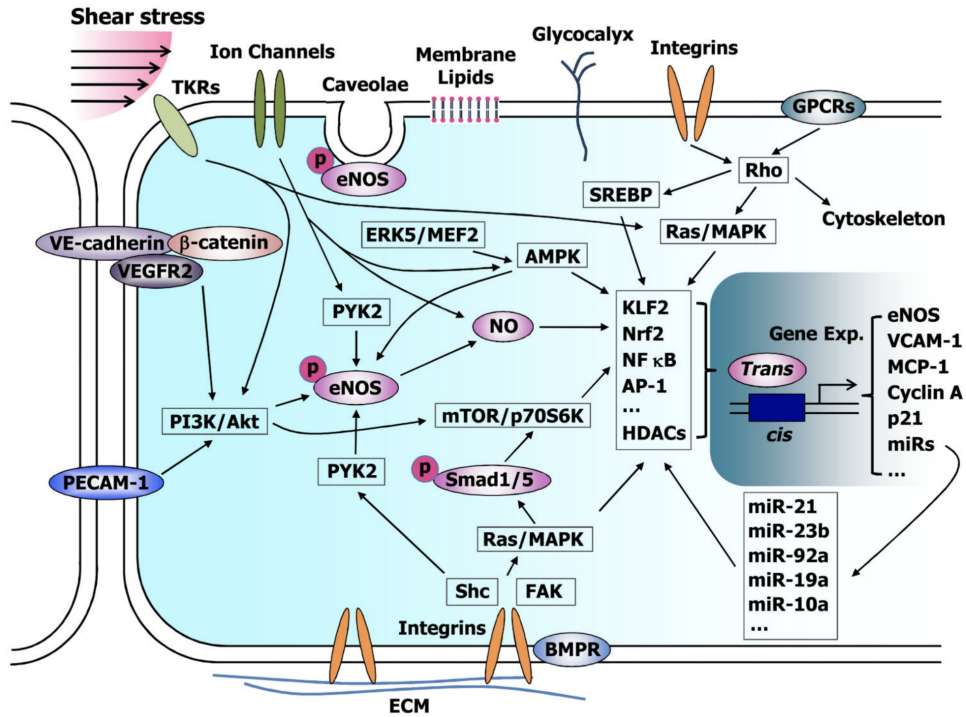
Figure 1.2: Mechanotransduction and signaling induced by shear stress.
Shear stress stimulates ECs through mechanosensors and cell membrane structures, such as ion channels, caveolae, membrane lipids, glycocalyx, integrins, tyrosine kinase receptors (TRKS) and intercellular junctions (e.g. VE-cadherin, PECAM-1). These then act through adaptor molecules such as Src homology 2 domain containing transforming protein 1 (Shc) to trigger the activation of signaling molecules like Ras, Rho, PI3K, and MAPKs to activate eNOS, Smad1/5, and transcription factors like KLF2, NF-κB, and AP-1 to regulate functional genes as well as microRNAs (miRs). All these pathways work in concert to modulate EC biological and molecular functions. [5]

Atherosclerosis alone is rarely fatal; rather, it is thrombosis, the formation of blood clots, that leads to life-threatening clinical events like acute coronary syndromes and stroke. Possible causes may include elevated and modified low-density lipoprotein (LDL), free radicals from cigarette smoking, hypertension, diabetes mellitus, and genetic alterations. Initial fatty streaks are observed in childhood and may be present throughout a person's lifetime [6] [7].

In lesion-prone areas, lesions begin to develop under leaky and dysfunctional endothelium. Plasma molecules and lipoprotein particles enter the subendothelilal space where the lipoprotein oxidize and become cytotoxic, proinflammatory, and atherogenic. The endothelium becomes activated by the atherogenic stimuli and upregulate the expression of adhesion molecules like vascular cell adhesion molecule-1 (VCAM-1), intercellular adhesion molecule (ICAM-1), and E-selectin (SELE), to recruit monocytes. Such monocytes are essential to the development and exacerbation of atheroscelerosis, as they migrate into the intima and differentiate into macrophages, which take on inflammatory phenotypes in progressing lesions [8].

Early in atherogenesis, scavenging macrophages clear atherogenic lipoprotein from the intima, leading to foam intracellular lipid accumulation, also known as foam cell formation. During the progression of atherosclerosis, endothelial cells, macrophages, and smooth muscle cells die by apoptosis, causing a destabilizing lipid-rich core and a fragile fibrous cap that is prone to rupture.

A shift from a stable to an unstable plaque is an indicator in the severity of atherosclerotic disease. Angiogenesis is frequent in advanced atherosclerosis. Accumulation of cells within the growing plaque and decreased oxygen tension leads to increase of oxygen demand within the plaque, thus leading to hypoxia and correlating with the severity of the plaque. Hypoxia stimulates angiogenesis through upregulating hypoxia inducible factors (HIFs) and vascular endothelial growth factor (VEGF) expression, thus inducing neovascularization of the plaque to meet increase oxygen demand [9]. The new microvessels formed are fragile and leaky, and express factors such as VCAM-1 that results in the local extravasation of inflammatory cells, plasma proteins, and erythrocytes causing bleeding. The coexistence of angiogenesis and inflammation hence could mediate rapid plaque progressing [7].

Effects of shear stress on endothelial cells and implications for atherosclerosis Pulsatile blood flow is characterized by a positive mean flow rate, exerts pulsatile shear (PS) on the endothelium and is associated with an atheroprotective endothelial phenotype, with atherosclerotic plaques rarely developing in such regions over time. Disturbed flow is characterized by irregular flow patterns with little to no mean flow rate, exerts oscillatory shear (OS) and is associated with an atheroprone endothelial phenotype, with plaque frequently forming in these regions [10]. The net effect of PS is to upregulate atheroprotective genes and downregulate atheroprone genes, whereas the net effect of OS is the opposite.

Disturbed blood flow is one of the key elements that contribute to the development of atherosclerosis

in blood vessels. Disturbed blood flow is more prevalent in atheroprone regions of the arterial tree, which is characterized by branch points and curved areas, as compared to high laminar shear in relatively straight parts of the aorta. The association between atherosclerosis and shear stress has been explicitly established by previous studies [1], [11], [12] .

Cardinal signs of sustained inflammation include various histocompatibility antigens presented on ECs such as: inducible endothelial-leukocyte adhesion molecules such as SELE and VCAM-1; procoagulant molecules such as tissue factor, and secreted chemokines, such as interleukin-8 (IL-8) and monocyte chemotractant protein-1 (MCP-1). Together, all these events lead to a localized and temporally coordinated proinflamamtory endothelial phenotype at sites of inflammation that is detectable *in vivo* [13].

1.2 Histone modification

In eukaryotic cells, genetic structure is stored in a chromatin structure. The basic unit of a chromatin is a nucleosome, which is composed of 1.67 turns of DNA that wraps around 8 histones. These 8 histones are two copies of each core histone, H2A, H2B, H3 and H4. Chemical modification of N-terminal tails of histone proteins are subject to a wide range of modifications, such as acetylation, methylation, phosphorylation and ubiquitylation [14]. These modifications influence chromatin structure and gene function and differ depending on the type of modification and location. For example, such post translational modification either induces functional activity, or renders them inactive. In particular, this thesis focuses on the methylation of histone H3 at lysine 9 (H3K9), which is important for silenced transcription and heterochromatin structure.

There are three lysine methylation states: mono-, di- and trimethylation (me1, me2, and me3, respectively). None of these states change the electronic charge of the amino-acid side chain and thus are considered to be exerted by effector molecules that specifically recognize the methylated site [15]. Histone lysine modification confer active or repressed transcription depending on their positions and methylation states. For example, H3K4, H3K36, and H3K79 methylations are considered to mark active transcription, while H3K9, H3K27, and H4K20 methylations are considered to mark silenced transcription.

In humans, repeat-rich constitutive heterochromatin is marked by H3K9me2 and H3K9me3, and are catalyzed by a family of SET-domain containing methyltransferases. SETDB1 and related enzymes SUV39H1and SUV39H2 contribute to both H3K9me2 and H3K9me3. H3K9me2/3 are bound by chromodomain of heterochromatin protein 1 (HP1), which self-oligomerize and recruit repressive histone modifiers, thus contributing to heterochromatin compaction and spread [16].

As the epigenome is influenced by many interacting external factors, understanding its modifications

is thought to be helpful in comprehending diseases of multifactorial genesis, such as atherosclerosis.

2   Materials and Methods

2.1   Introduction

Pulsatile shear stress (PS) and oscillatory shear stress (OS) flow patterns were applied to human umbilical vein endothelial cells (HUVECs) for 24 hours. Chromatin immunoprecipitation followed by high-throughput sequencing (ChIP-seq) was used to determine enrichment for histone modification on a genome-wide scale.

In a systems biology analysis, we explore the functional response of endothelial cells to shear stress across PS and OS conditions through genes implicated in various cellular and tissue function, such as oxidative stress, inflammation, proliferation, and migration.

The goal of a ChIP-seq experiment is to identify genomic regions that interact with a histone mark of interest. The bindings appear as regions with high read densities, referred to as peaks.

High-throughput sequencing is performed randomly on either end and does not cover the complete length of the enriched DNA fragments. This is why reads mapping to the forward and the reverse strange from a characteristic bimodal distribution.

Depending on the type of protein, the shape of the ChIP-seq signals can be sharp or broad. Histone marks span several nucleosomes that are not specifically positioned on the DNA, but rather depend on the position of the neighboring transcription factors. DNA fragments covering the same region correspond to several nucleosomes that can be loosely positioned on the DNA. This is why ChIP-seq signals for H3K9me2/me3 appear as broad regions of enrichment that can reach several kilobases [17].

2.2   Cell culture and shear stress experiment

ECs in OS conditions are characterized by a rounded shape and no obvious directional growth, compared to ECs in PS conditions, with morphology that show cell elongation in the direction of shear stress.

Human umbilical vein endothelial cells (HUVECs) were cultured in medium M-199, which consists of 10% fetal bovine serum (FBS), 1% sodium pyruvate (NaPyu), 1% penicillin-streptomycin, 10% endothelial cell growth medium (ECGM), and 1% L-glutamine. Cells from passage 3-6 were used.

Mechanisms of EC response to specific shear stress patterns are inferred from signalling and transcriptional measurements. A parallel-plate flow chamber is used to study such response *in vitro*. This device consists of a polycarbonate base plate, a gasket, and a glass slide with EC monolayer. The base plate has inlet and outlet ports where fluid flows in and out of the device, passing over and exerting fluid shear stress on the EC.

Culture medium is used as fluid and flow is induced using an external pump. The pumps can simulate pulsatile shear stress (PS) of $12 \pm 4 \, \mathrm{dyn/cm^2}$ and oscillatory shear stress (OS) of $0.5 \pm 4 \, \mathrm{dyn/cm^2}$. These flow rates were maintained for 24 hours.

2.3 Chromatin immunoprecipitation followed up high-throughput sequencing (ChIP-seq)

Chromatin immunoprecipitation followed up high-throughput sequencing (ChIP-seq) is a technique used to determine *in vivo* binding sites of chromatin associated proteins and enrichment for specific histone modifications on a genome-wide scale.

ChIP methodology involves protein-DNA crosslinking, fragmentation of the cross-linked chromatin, and subsequent immunoprecipitation. The DNA fragments isolated with the target protein then can be identified by high throughput DNA sequencing, and standard or quantitative PCR can be used to identify whether a particular DNA sequence is associated with the protein of interest. The Magna ChIP kit protocol was used to perform the ChIP experiment as follows:

(A) **In vivo cross-linking and lysis** Cells were fixed in 1% formaldehyde by mixing 225 μl 37% formaldehyde to 10 ml of growth medium and incubated for 10 minutes. 1 ml of 10X glycine was added to quench the unreacted formaldehyde for 10 minutes and incubated in 4°C for 3 minutes.

0.5X Protease Inhibitor Cocktail II (2.5 μl for every 1ml PBS) was added to each dish and cells were washed with 1X PBS. A cell scraper was used to collect cells from each dish, and then centrifuged at 4°C at 10000 rpm for 3 minutes and the supernatant removed.

(B) **Sonication of isolated chromatin to shear DNA** A Bioruptor (Diagenode, New Jersey, USA) was used to sonicate the cell lysate at 4°C, with 8 cycles. Cycle condition is 30 seconds on and 30 seconds off. The target size is estimated to be 150 bp per protocol settings. Cell lysate is then centrifuged at at 4°C at 10000 rpm for 5 minutes to remove insoluble material.

(C) **Immunoprecipitation (IP) of cross linked protein/DNA** Dilution buffer containing protease inhibitors are prepared as follows: For each IP, 450 μl of Dilution Buffer and 2.25 μl of Protease Inhibitor Cocktail II are used.

5μl of the supernatant (10%) is removed as 'Input' and stored at 4°C until Section (D) (Elution of Protein/DNA complexes and reverse cross-links of protein/DNA complexes to free DNA).

450 μl of the Dilution Buffer containing Protease Inhibitor Cocktail II was added to each sample of chromatin, along with 20μl of the A/G magnetic beads. 2 μl of antibody H3K9me3 (Abcam, CITE)

was added for each sample and incubated overnight at 4°C with rotation.

A/G magnetic beads were pelleted with a magnetic separator and supernatant discarded. The A/G magnetic beads/chromatin complex were washed by resuspending the beads in 500 μl of each of the cold buffers in the order listed below, then incubated for 5 minutes at 4°C with rotation, followed by magnetic separation and removal of the supernatant.

1. Low Salt Wash Buffer

2. High Salt Wash Buffer

3. LiCl Wash Buffer

4. TE Buffer

(D) **Elution of Protein/DNA complexes and reverse cross-links of protein/DNA complexes to free DNA** The final elution buffer (100 μl of ChIP Elution Buffer and 1 μl of Proteinase K) is prepared for each sample, including the input samples, and incubated at 62°C for 2 hours, followed by 95°C for 10 minutes. After cooling to room temperature, the beads are separated and the supernatant collected.

(E) **DNA purification** DNA purification was conducting using QIAquick PCR Purification Kits (QIAGEN, CITE). 5 volumes of Buffer PB was added to 1 volume of each sample. DNA is bound and applied to the QIAquick column and centrifuged at 13000rpm for 1 minute at 4 °C. Flow-through was discarded, sample is washed with Buffer PE and centrifuged at 13000rpm for 1 minute at 4 °C. Flow through was discarded again and centrifuged to remove buffer PE at 14000rpm for 1 minute at 4 °C.

To elute DNA, 30 μ Buffer EB was added to each sample and heated at 37 °C for 10 minute, then centrifuged at 14000 rpm for 3 minutes at 4 °C.

The preparation of various sequencing libraries and sequencing by use of an Illumina HiSeq 2000 sequencer were performed in the IGM Genomics Core, University of California, San Diego.

2.4   Western blot

Resolving gel was prepared as follows:

1. Water

2. 30% acrylamide mix

3. 1.5M Tris (pH 8.8)

4. 10% SDS

5. 10% ammonium persulfate

6. TEMED

Stacking gel was prepared as follows:

1. Water

2. 30% acrylamide mix

3. 1.5M Tris (pH 6.8)

4. 1% SDS

5. 10% ammonium persulfate

6. TEMED

Samples were heated to 95 °C for 5 minutes and quenched in ice. 200 μl of each sample and 5μl of the rainbow protein marker were loaded into separate wells, and ran at 60 V for 30 minutes.

After loading and running the gel, the proteins were transferred from the gel to the membrane, and prepared as shown in Figure 2.1 at 300 mA for 2.5 hours.

Blot was incubated in blocking agent (0.1% TBST and 5% BSA) with agitation for 30 minutes at 4 °C. Blot was then placed into primary antibody solution with agitation overnight at 4 °C, rinsed twice with TBST buffer, and placed in second antibody solution with agitation at room temperature for 1 hour. Primary antibody used was mouse polyclonal to H3K9me2 and rabbit to H3K9me3 (Abcam), and mouse and rabbit second antibody-conjugated HRP were used to recognize the first antibody, respectively. After incubation with antibodies, the blot was rinsed with TBST buffer and images acquired with fluorescent imaging. α-tubulin was used as normalization.

2.5 Immunostaining

The samples were placed in a 50°C oven for at 30 minutes, then deparaffinized in 100% xylene for thrice for 10 minutes each. The samples were then hydrated in 100%, 95%, 70%, 50% ethanol for 10 minutes each, and finally 1x PBS twice for 5 minutes. For antigen retrieval, the samples were immersed in a water bath of 10mM sodium citrate buffer with 0.05% Tween for 15 minutes after the buffer has reached 95°C. The samples were then rinsed with PBS thrice, and blocked with Blocking Reagent for 1 hour in 4°C. Samples were incubated with primary antibody in 4°C overnight, and secondary antibody for 1 hour at room
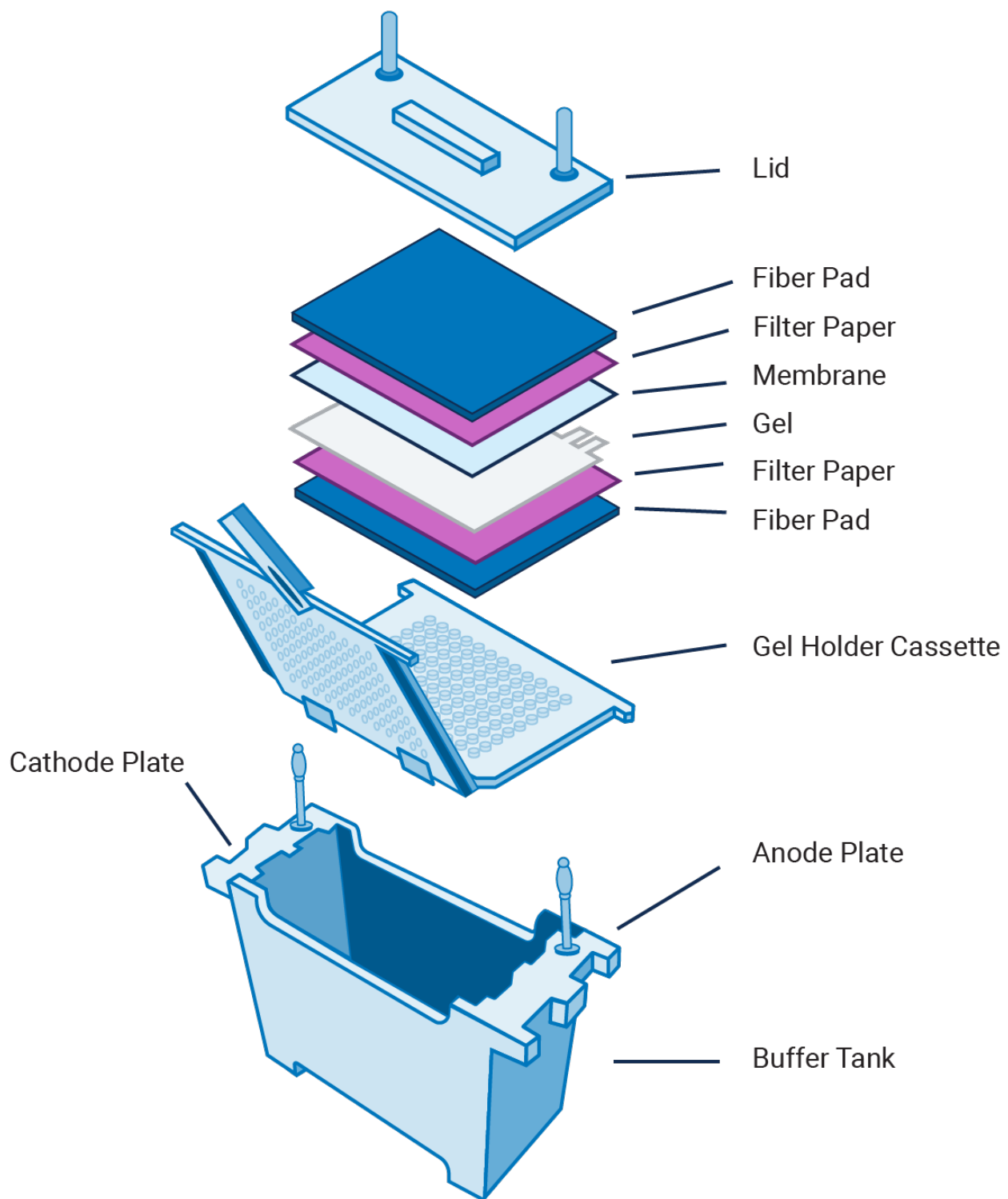
Figure 2.1: Wet transfer process in Western blot

temperature. The samples were then mounted with coverslip and examined using fluorescence microscopy.

2.6 Systems Biology

Rosalind

Sequencing data was analyzed by Rosalind (https://rosalind.onramp.bio/), with a HyperScale architecture developed by OnRamp BioInformatics, Inc. (San Diego, CA). Reads were trimmed using cutadapt. Quality scores were assessed using FastQC. Reads were aligned to the Homo sapiens genome build hg19 using bowtie2. Per-sample quality assessment plots were generated with HOMER and Mosaics. Peaks were called using MACS2. Peak overlaps and differential binding were calculated using the DiffBind R library. Differential binding was calculated at gene promoter sites. Read distribution percentages, identity heatmaps, and FRiP plots were generated as part of QC step using ChIPQC R library and HOMER. HOMER was also used to generate known and *de novo* motifs and perform functional enrichment analysis of gene ontology.

MACS2

Since histone mark data show broad enrichment of signal and require identification of large regions, peak finders like MACS2 [18] are appropriate for broad regions. Briefly, it first removes all duplicated reads. The fragment size is estimated using double distribution of forward and reverse reads from highly enriched regions. It extends all reads to the estimated fragment size and scales ChIP and input to the same sequencing depth. This scaling normalizes to the total number of mapped reads in the library. It then scans the distribution of fragments along the genome using a sliding window to score regions. To do so, it compares the enrichment in ChIP vs control samples, and calculates a significance score using local Poisson distribution. Finally, the Benjamini-Hochberg procedure is used to correct for multiple testing. As a default, it returns peaks with a minimum q-value score of 0.05. [17]

DiffBind

The R Bioconductor package DiffBind provides functions for processing ChIP-seq data, including peaksets that have been identified by ChIP-seq peak callers, such as MACS2 used in this analysis. The main use of DiffBind is used to identify sites that are differentially bound between two or more sample groups. It includes functions that supports the processing of peak sets, including overlapping and merging peak sets, and identifying statistically significantly differentially bound sites. Such identification is based on evidence of binding affinity, which is measured by differences in read densities.

The following terminology will be used to compare peaks with other conditions: PS vs OS, PS vs C, OS vs C.

Gene Ontology

Such high-throughput studies result in a set of genes that are bound by the same factor (H3K9me2 and H3K9me3 respectively). It is difficult to determine how, or even if, the genes interact with each other by just reviewing the list of genes obtained from the prior experimental studies. Computational approaches to understand the features and functional significance of these genes are therefore an important part in understanding the features of such genes. A practical way to understand the question of "what is going on?" is to perform gene-category analysis, which is to identify whether a specific set of genes share some biological features that distinguish them from the set of all genes. These biological features can include biological processes, components or structures in which individual genes and proteins are known to be involved in, as well as certain pathways where gene products are involved in at different time points.

There are two advantages to understanding high-throughput data on a functional level. First, grouping tens of thousands of such genes by pathways can reduce the complexity to several hundred pathways for further analysis. Second, identifying active pathways that are unique to each experimental condition provides more explanatory power than just a simple list of genes [19].

Gene-category analysis is the grouping of all genes with similar features into a list of gene categories (or ontologies). There are two important factors involved in the categorization such genes: categories depending on a database and a statistical method to identify categories. The definition of similar features depends on the provider of the categories [20]. For example, if Gene Ontology (GO) is the source of categories, genes will be grouped according the terms provided by such a database. We can also use Kyoto Encyclopedia of Genes and Genomes (KEGG) database, where the genes are grouped according to the pathways they are involved in. These categories are named annotations, or ontologies. Various tools used to define these categories make use of different statistical methods, which will be mentioned below.

A way of understanding the biological meaning of a gene set is to consider what processes or functions are over-represented (enriched) or under-represented (depleted) amongst genes in the set. This is by comparing the distribution of the terms within a set of interest after systemic mapping of genes to their annotations. The significance of enrichment or depletion scores is based on various statistical models. It is inferred that such enriched terms describe some important underlying biological process or behavior [21].

13

3 Results

3.1 PS increases H3K9me2 and H3K9me3 levels in HUVECs

In order to explore the functional relationship between histone modifications and shear stress, the levels of H3K9me2 and H3K9me3 for three conditions respectively: control (C), pulsatile shear (PS), and oscillatory shear (OS) were analyzed by Western blot (Figure 3.1). Figure 3.2 shows that both H3K9me2 and H3K9me3 were significantly increased under PS relative to control; and no significant changes were observed for OS relative to control. This shows that exposure of PS for 24 hours induces the levels of H3K9me2 and H3K9me3 in HUVECs.
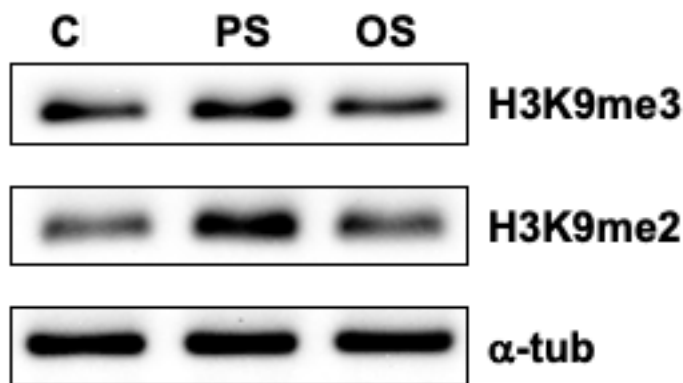

Figure 3.1: Western blot results
H3K9me2, H3K9me3, and α-tubulin in human umbilical vein endothelial cells (HUVEC) for control (C), pulsatile shear (PS), and oscillatory shear (OS) conditions.

3.2 Quality control of H3K9me2 and H3K9me3 ChIP-seq data

Replicates A way to assess concordance of peak calls between replicates is to make use of a statistical procedure to compare a pair of ranked lists of peaks called Irreproducible discovery rate (IDR) [22]. This measure provides a score that estimates the probability that each pair of peaks is reproducible through a copula mixture model. IDR however is only appropriate for transcription factors (narrow peaks), since histones (broad peaks) produce a much smoother and variable range of signal; thus making use of a cutoff that is based on rank consistency from MACS2 makes makes it too conservative.

For broad peaks, often one peak overlaps with multiple small peaks of another replicate. When this occurs, all these small peaks are lumped as one peak and the most substantial significance of these small peaks is used as the significance of the lumped peaks [23]. As such, estimating the reproducibility across
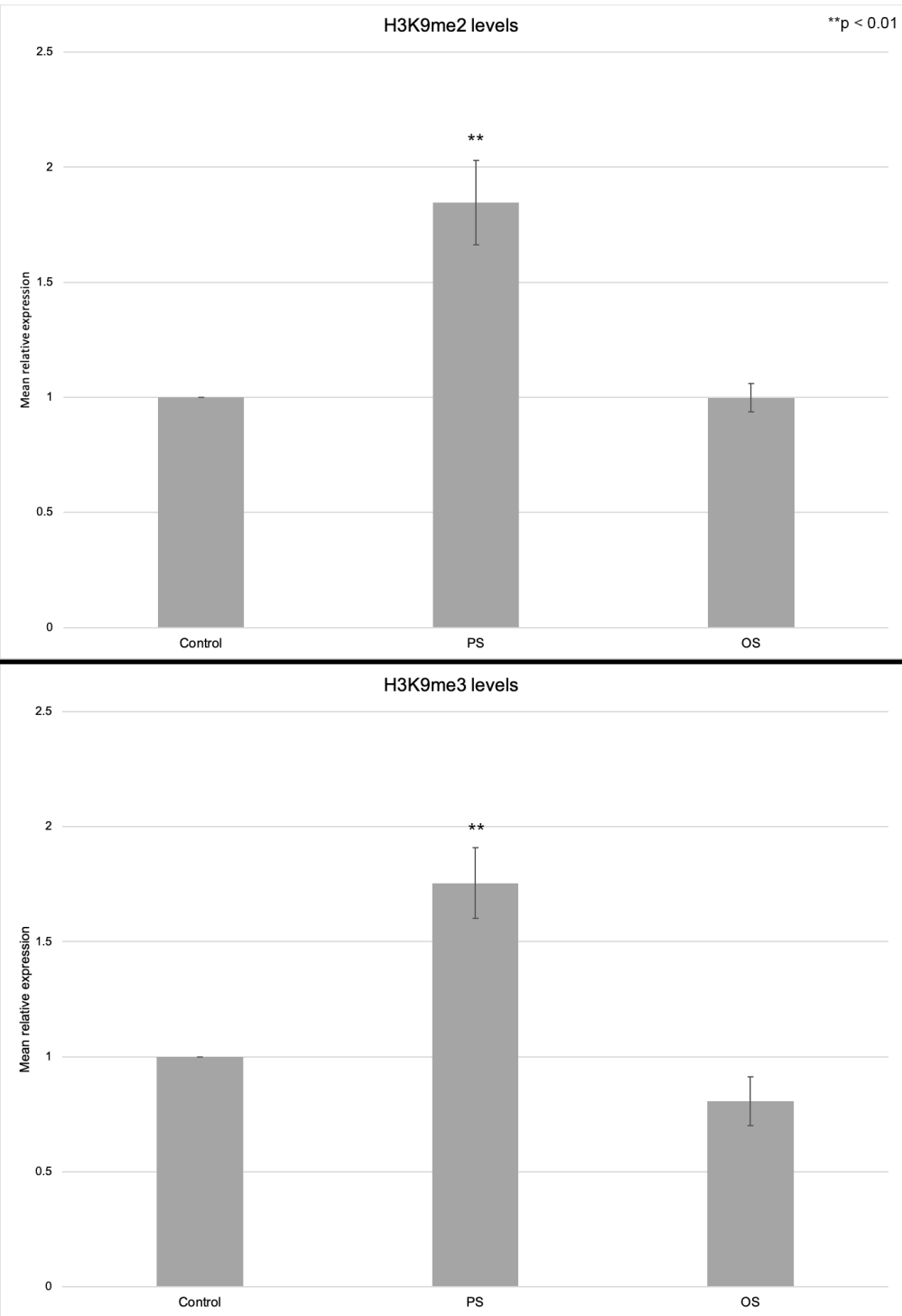
Figure 3.2: H3K9me2 and H3K9me3 levels.
Values are mean +/- standard error. Number of samples = 3. Significant differences (p ¡ 0.01, t-test) between PS and C, as well as OS and C are indicated by a (**). Control (C), pulsatile shear (PS), and oscillatory shear (OS).

Table 3.1: ChIP-seq alignment results.

Q30: The percentage of reads with a quality score of 30 or higher. This value is an average across the whole read length, and error rate increases towards the end of the reads; Bases trimmed: The number of bases removed by trimming (and percent of total bases in sample); % Aligned reads: the number of reads that aligned to reference genome/total number of reads; % Duplicated reads: Percentage of aligned reads that are duplicates.

Sample	Reads	Q30	# Reads too short	% Aligned reads	% Duplicated reads	Peaks
ME2 C	32723507	81	0	89	4	3066
ME2 OS	26413535	74	0	86	3	8867
ME2 PS	21120618	74	0	87	4	10228
ME3 C	22940144	84	0	88	7	4459
ME3 OS	21038414	76	0	88	4	4014
ME3 PS	31642623	75	0	88	4	51174

replicates is difficult since peak boundaries and ranking measures are unstable.

Sequencing depth is defined as the number of uniquely mappable reads. H3K9me2/me3 usually occurs in repeat-enriched regions, hence the number of uniquely mappable reads is substantially lower than in other modifications [24]. After identifying the sequencing depth for each of the replicates, we have decided to pool replicates together to obtain sufficient information.

ChIP-seq peaks Bowtie2 was used to align the sequencing reads to the reference genome as described in the previous section, and the alignment results are presented in Table 3.1. Sequencing depth for each of the pooled samples are around 20 to 30 million reads, which is sufficient to identify binding sites in a sample. PS conditions have the largest numbers of peaks for each sample. For PS conditions, in H3K9me2 samples, 10228 peaks were found. In H3K9me3 samples, 51174 peaks were found. We must note that these peaks are not a comparison between conditions, but rather the number of peaks found in each sample sequence. These values are used in quality control where the number of peaks can be observed as expected. Further analysis was conducted to compare the peaks across different conditions.

Table 3.2: Percentage of fraction of reads in peaks (FRiP).

Sample	% in peaks
ME2 C	0.289
ME2 OS	0.323
ME2 PS	0.265
ME3 C	0.518
ME3 OS	0.338
ME3 PS	0.209

FRiP FRiP (Fraction of Reads in Peaks) is a quality measure conveying the percentage of all reads that fall in regions of local enrichment (Peaks). FRiP scores are correlated with ChIP efficiency as well as with replicate reproducibility. Broad-source factors like H3K9me2 and H3K9me3 often have marginal or truly low scores (Table 3.2) due to the relative low peak intensity, or height, even if samples are of high quality [25].

Distribution of peaks Approximately 60% of all peaks are found in the intergenic region for H3K9me2 and H3K9me3 in PS and OS conditions, 30% in introns, and the rest in other genomic regions as shown in Figure 3.3. In mammalian cells, H3K9me2 and H3K9me3 are enriched in repressed constitutive heterochromatin, which are repetitive regions where silencing is universal across all cells [26], [16]. The relative enrichment of ChIP-seq reads within these regions correlate to the genomic proportion and indicates that the expected genomic distribution was captured [17].
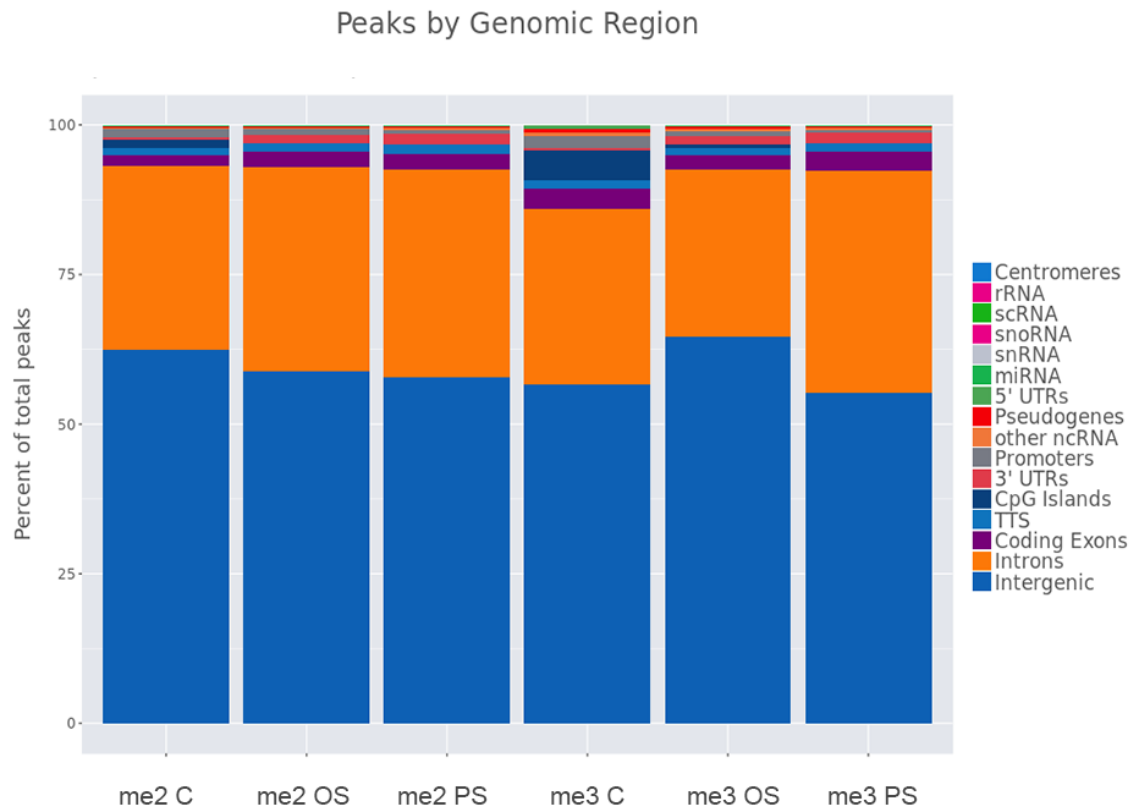
Figure 3.3: Peak distribution across gene-related and regulatory features of genome.
Each column sums up to 100%. Genomic regions include: GpG islands, intergenic regions, introns, protein-coding exons ("Coding Exons"), 5' UTR exons, 3' UTR exons, promoters, transcription termination sites (TTS), centromeres, pseudogenes, non-coding RNAs, microRNAs (miRNA), small conditional RNAs (scRNA), small nucleolar RNAs (snoRNA), small nuclear RNAs (not including snoRNA) (snRNA), ribosomal RNA (rRNA), and other non-coding RNA (ncRNA).

3.3 Functional analysis of atheroprotective PS-annotated genes in HUVECs after 24 hours

Peak numbers The number of peaks found after comparison of different conditions as calculated by diffBind are shown in Figure 3.4 for H3K9me2 and H3K9me3 in PS, OS, and C conditions. These peaks will then be used for bioinformatics analysis.

Binding heatmaps Heatmaps are used to show the pattern of binding at the overlapped locations as shown in the Venn diagrams (Figure 3.4). The binding heatmap displays the read coverage density, with each row corresponding to the average peak profile for a single peak averaged within a group, and ranked by the strength of the signal.

H3K9me2. Binding heatmap of H3K9me2 shows a significantly large proportion of transcription start sites under PS conditions compared with C conditions. This is similar for OS compared to C conditions. Binding sites are roughly divided equally between PS and OS conditions (Figure 3.5).

H3K9me3. Binding heatmap of H3K9me3 shows a significantly large proportion of binding sites under PS conditions compared with C conditions. Similarly, this can be seen under PS conditions compared with OS and C conditions (Figure 3.6).

H3K9me2 PS vs OS vs C

ME2 PS 8453 · 746 · ME2 OS 7122 · 771 · 236 · 203 · ME2 C 1836

H3K9me3 PS vs OS vs C

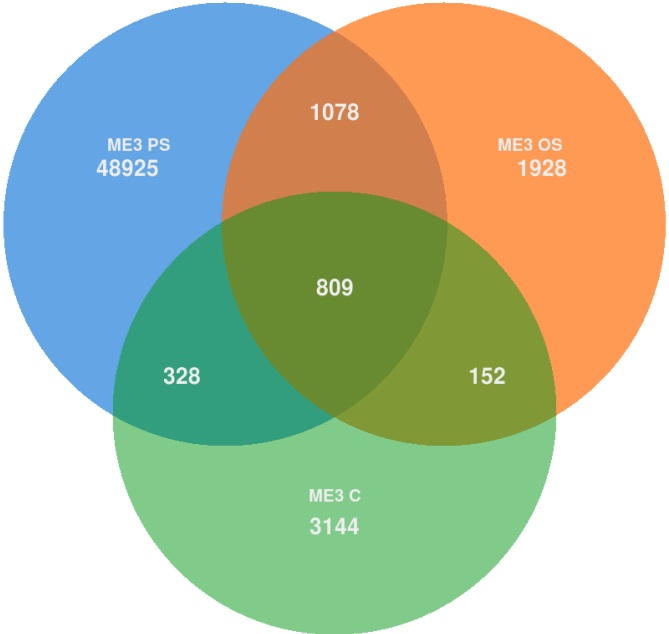ME3 PS 48925 · 1078 · ME3 OS 1928 · 809 · 328 · 152 · ME3 C 3144

Figure 3.4: Number of peaks found in the following conditions: PS, OS, C.
Top: H3K9me2, bottom: H3K9me3. Intersections in the diagram shows the overlap of genes found in each condition.
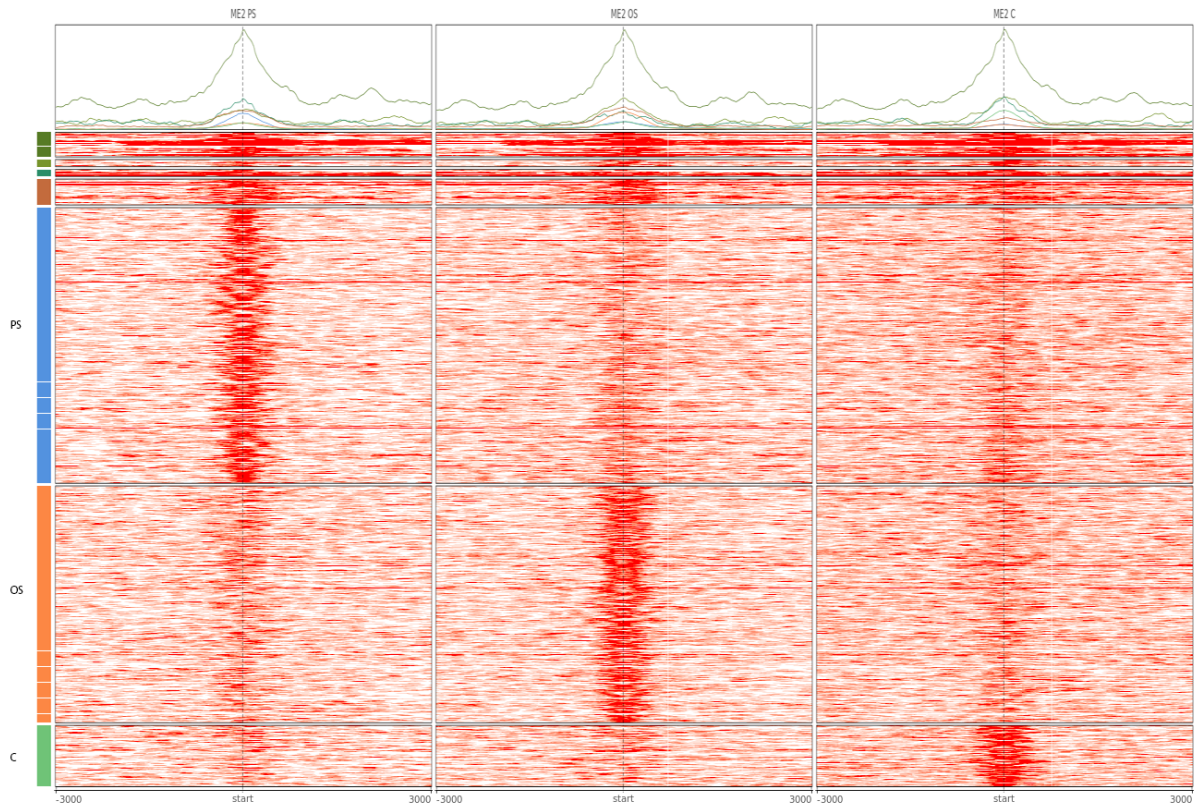
Figure 3.5: H3K9me2 binding heatmap.

Distance in binding heatmap is ± 3000 bases on both sides, centered around the binding sites. Colored bars on the left are in reference to Figure 3.4.
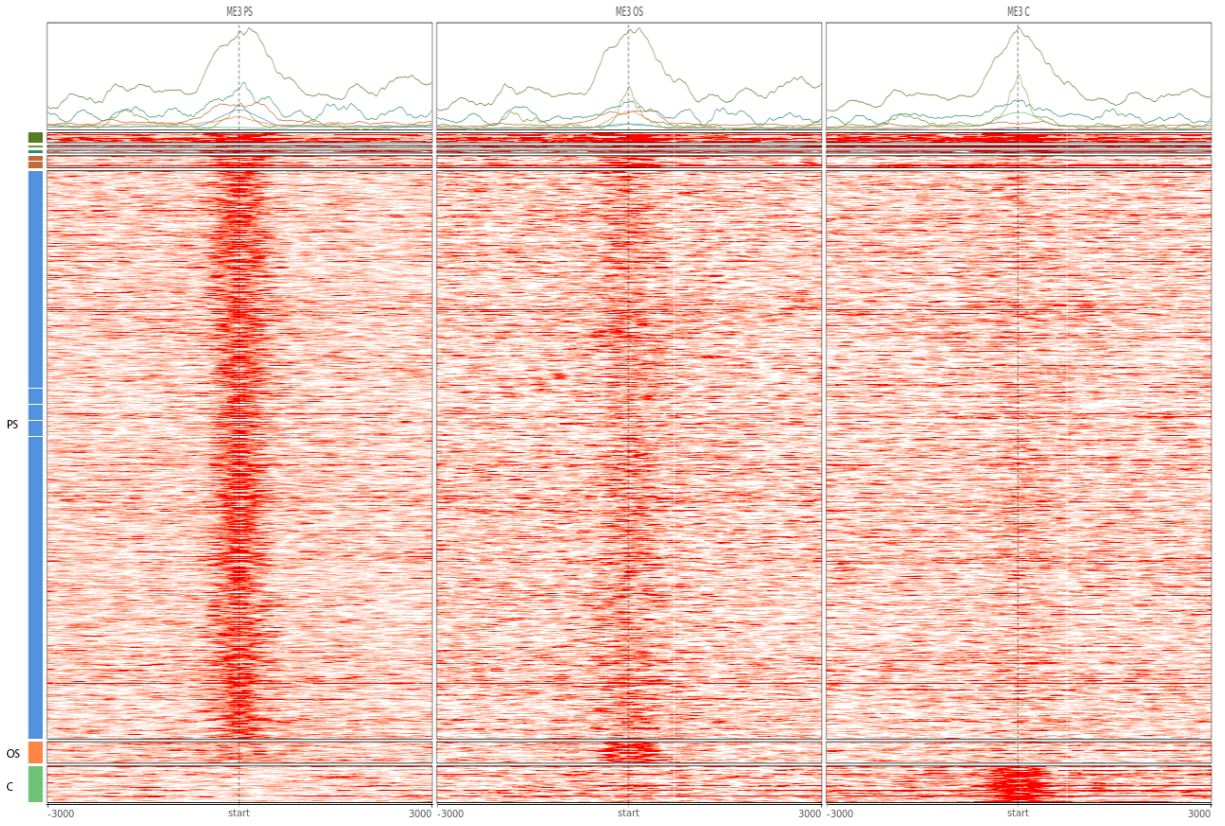
Figure 3.6: H3K9me3 binding heatmap.

Distance in binding heatmap is ± 3000 bases on both sides, centered around the binding sites. Colored bars on the left are in reference to Figure 3.4.

3.4 Gene ontology classification of PS genes after 24 hours of treatment

PANTHER functional classification was used to categorize the H3K9me2 and H3K9me3 ChIP-seq peaks into various categories. The categorization is based on Gene Ontology categories of Biological Process, Cellular Component, and Molecular Function.

Figure 3.7 and Figure 3.8 show the percentage of genes from ChIP-seq peaks in each ontology under different conditions for H3K9me2 and me3 respectively. The largest percentage of genes are under the term "Cellular Process", which is the parent term for other terms such as cell cycle, cell adhesion, signal transduction. Some other categories of interest involve response to stimulus, metabolic processes, and biological regulation. The results of ontologies are similar for H3K9me2 and me3.

Such visualization allows us to obtain a broad understanding of preliminary classification in order to make predictions about the functions of genes that are implicated in histone modification. Further analysis is needed to reveal enhanced categorization of the genes in detail.
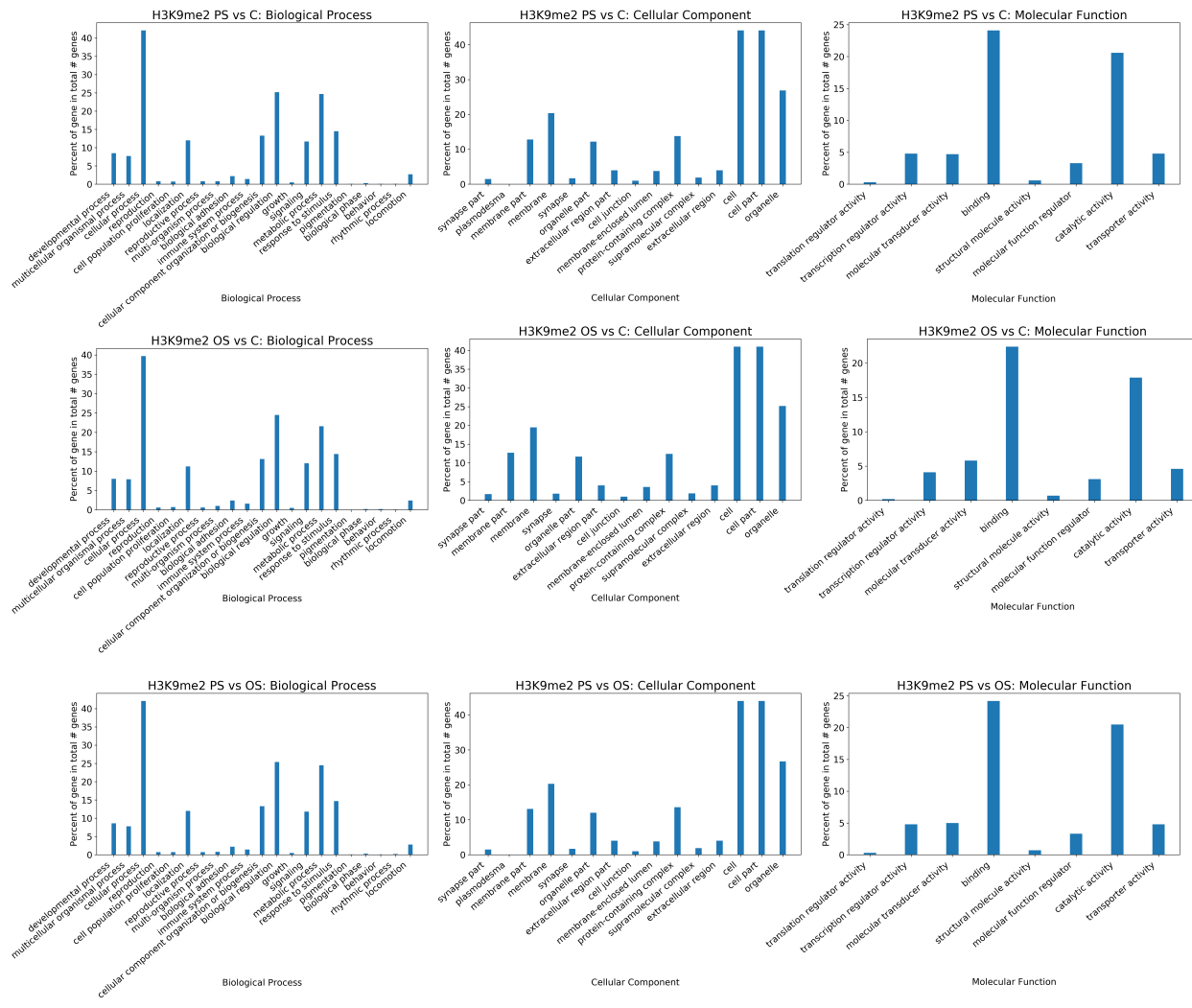
Figure 3.7: PANTHER classification: H3K9me2.

Top: PS vs C, Middle: OS vs C, Bottom: PS vs OS. Gene ontology categories include: Biological Process, Cellular Component, and Molecular Function.
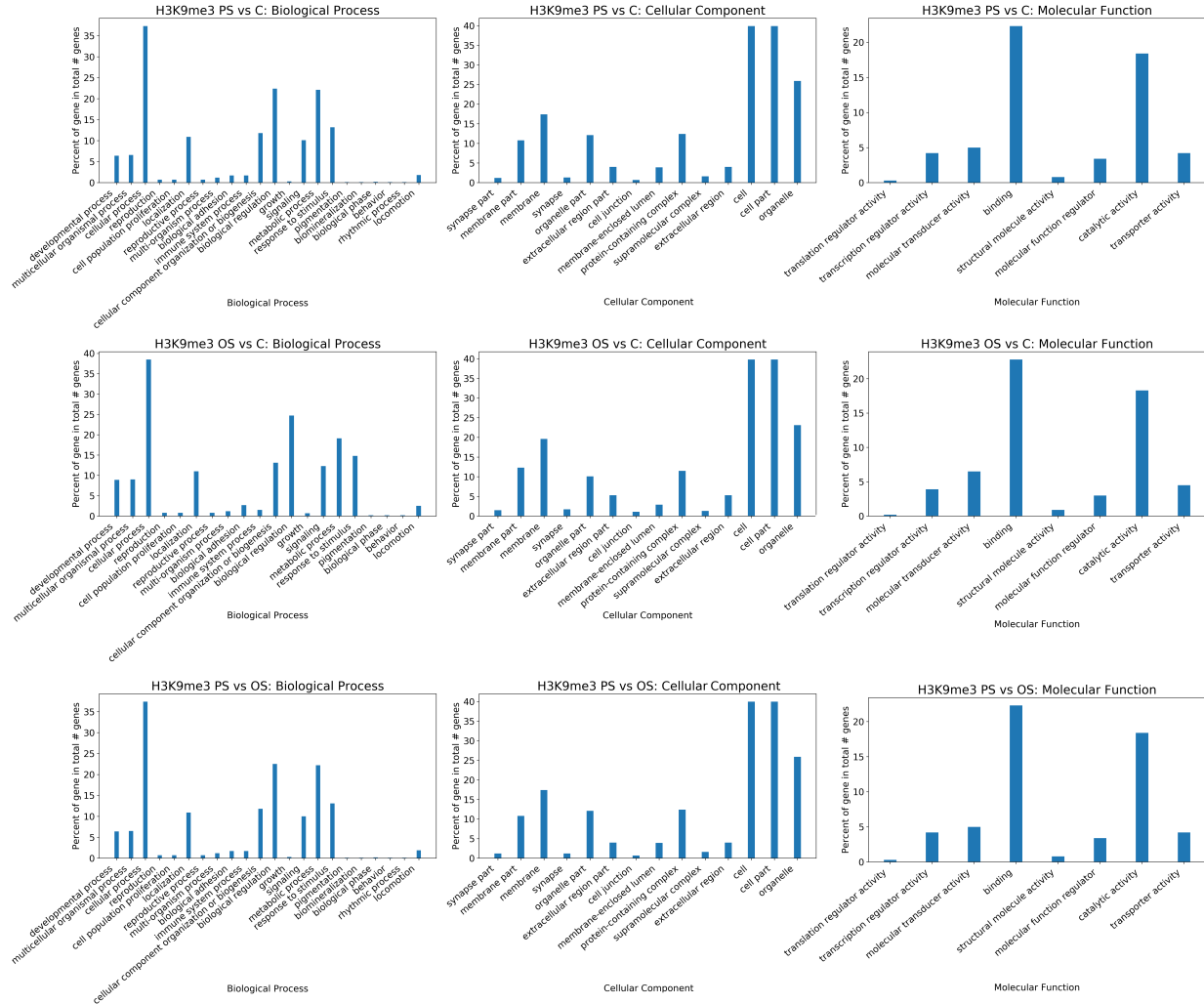
Figure 3.8: PANTHER classification: H3K9me3.

Top: PS vs C, Middle: OS vs C, Bottom: PS vs OS. Gene ontology categories include: Biological Process, Cellular Component, and Molecular Function.

3.5 Enrichment terms of PS genes show H3K9me2- and H3K9me3-induced TGF-β, GPCR, MAPK, and other signaling events

Following the classification of genes conducted by PANTHER, we can also identify which enrichment terms are more significant for H3K9me2 and H3K9me3. The aforementioned computational pipeline allows us to quantify the significance of each enrichment term through p-values. Enrichment terms found only in PS conditions associated with biological processes and molecular functions show the classification of such genes. The p-values of some enrichment terms may be low due to the lack of replicates. However, such values may not be significant when conducting exploratory analysis.

H3K9me2 For biological processes (Figure 3.9) in both PS vs OS and PS vs C conditions, a lot of the implicated terms were involved in nervous system development. This shows that PS peaks compared to both OS conditions and C conditions respectively do not differ significantly. However, across such differential analysis, such results were not informative in understanding the biological processes associated in endothelial cells. As for molecular function (Figure 3.10), pathways such as signal transducer with serine/threonine kinase activity, G-protein coupled receptor activity, signal transducer activity, which are implicated in the mechanism in signal transduction of shear stress into intracellular signals in ECs.

A look to some enrichment terms in Pathway Interaction Database (Figure 3.11) shows that in both H3K9me2 PS vs OS and PS vs C conditions, EphrinA-EPHA pathway was shown to be an enrichment term. Studies have shown that the Eph and ephrins family of receptor tyrosine kinases is associated with an inflammatory response and their pro-inflammatory association with atherosclerotic plaque formation [27], [28]. ErbB4 signaling events were implicated. A study conducted by Shakeri *et al.* [29] has shown mice cardiac and vascular endothelial cells produce neuregulin-1 (NRG-1), which acts through ErbB4 tyroskine kinase receptors expressed on ECs in a paracrine and autocrine fashion in response to inflammation, hypoxia, and oxidative stress to inhibit cellular senescence *in vitro* and *in vivo*. Another study conducted by Xu *et al.* [30] has also shown the anti-atherosclerotic role of NRG-1 in ApoE-/- mice. Stimulation of HUVEC with an ErbB4 ligand has induced rapid calcium fluxes, receptor tyrosine phosphorylation, and cell proliferation [31].

These various pathways suggest that there is activation of signaling events that allows for the transmission of mechanical stress into the nucleus for histone modification, as well as promoting cell fate decisions towards proliferation and inflammation in response to mechanical stimulation.
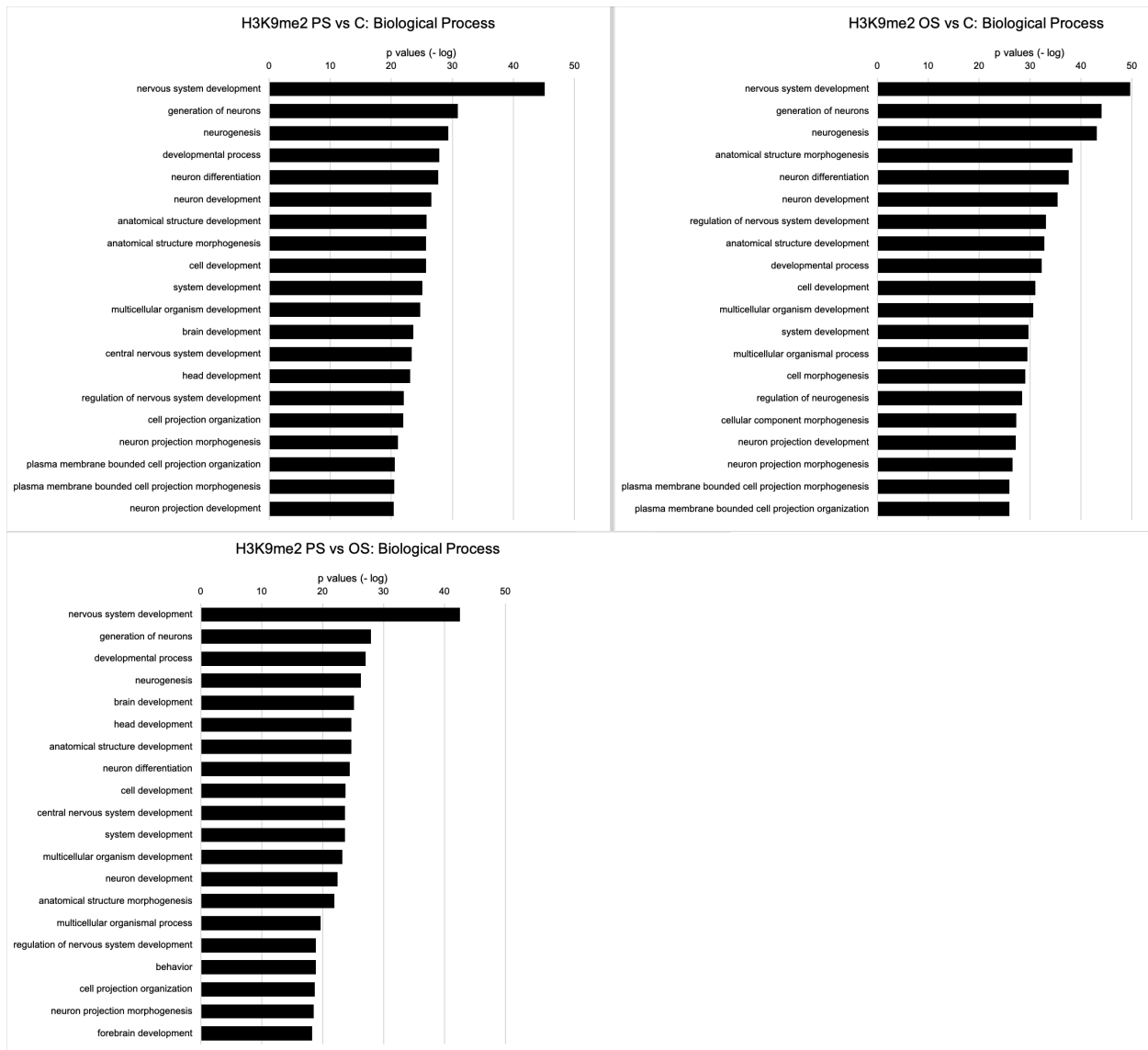
Figure 3.9: Gene Ontology: Biological Processes. H3K9me2

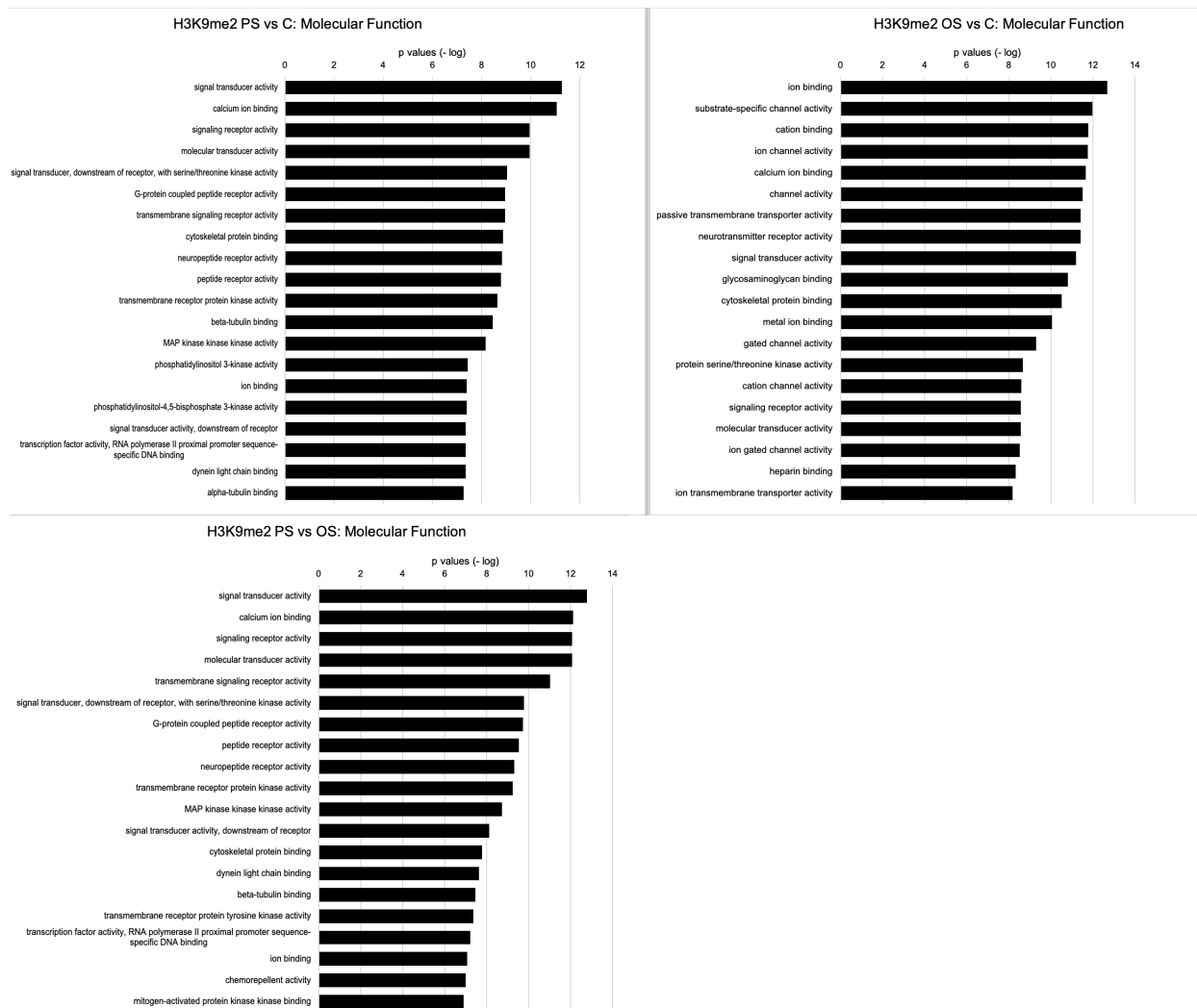P-values of top 20 enrichment terms for PS vs C, OS vs C, and PS vs OS.

Figure 3.10: Gene Ontology: Molecular Function. H3K9me2

P-values of top 20 enrichment terms for PS vs C, OS vs C, and PS vs OS.
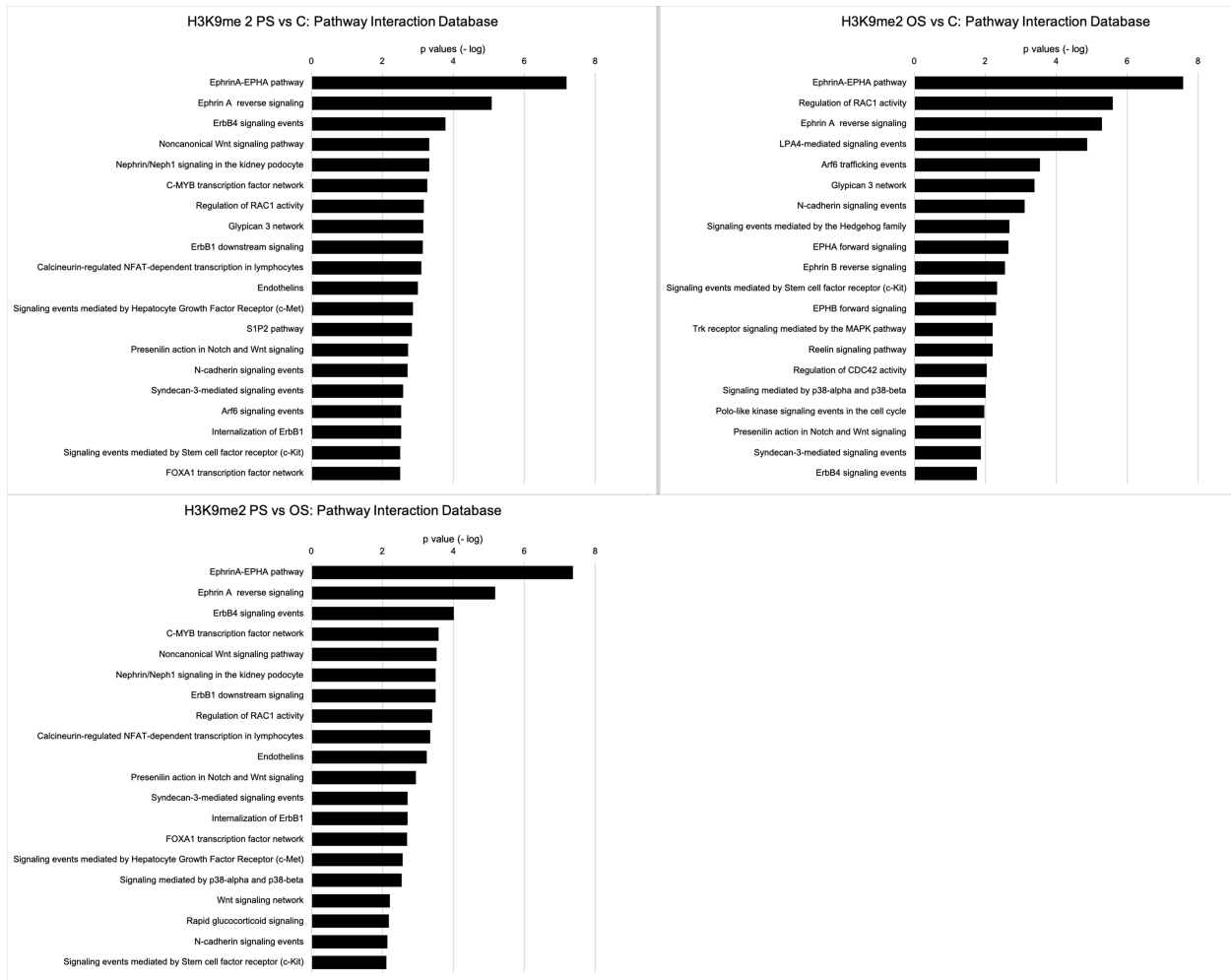
Figure 3.11: Pathway Interaction Database. H3K9me2

P-values of top 20 enrichment terms for PS vs C, OS vs C, and PS vs OS.

H3K9me3 For biological processes (Figure 3.12), some interesting classifications include detection of stimulus involved in sensory perception, where sensory stimulus is received and converted into a molecular signal, as well as G-protein coupled receptor signaling pathway. For molecular functions (Figure 3.13), some insight to the mechanism that underlies H3K9 methylation through shear stress can be seen from transmembrane signaling receptor activity, G protein-coupled receptor activity, p38 MAPK, and protein kinase activity, through the transmission of mechanical stress into the nucleus for epigenetic regulation. Protein kinase activity, G protein-coupled receptors, receptor tyrosine kinases (RTK) has been implicated in the link between shear stress and atherosclerosis [32], [33]. Such enrichment terms are similar for H3K9me3 PS vs OS and PS vs C conditions.

Another pathway of interest is the transforming growth factor beta (TGF-β) receptor signaling. This pathway has been shown to mediate protective effects of shear stress in HUVEC via induction of TGF-β signaling and downstream KLF2 and NO signaling, the classic mediator of the atheroprotective effects of shear stress [34]. Finally, signaling events mediated by T-cell protein tyrosine phosphatase (TCPTP) was also found. A study conducted by Mattila [35] shows that TCPTP is expressed in the HUVEC and in human endothelium *in vivo*, and TCPTP activity regulates VEGFR2-mediated proliferation and migration of HUVEC.

Similarly, these cascades are involved in the regulation of cell cycle progression, metabolism, survival, and apoptosis that are relevant in atherosclerosis[36].
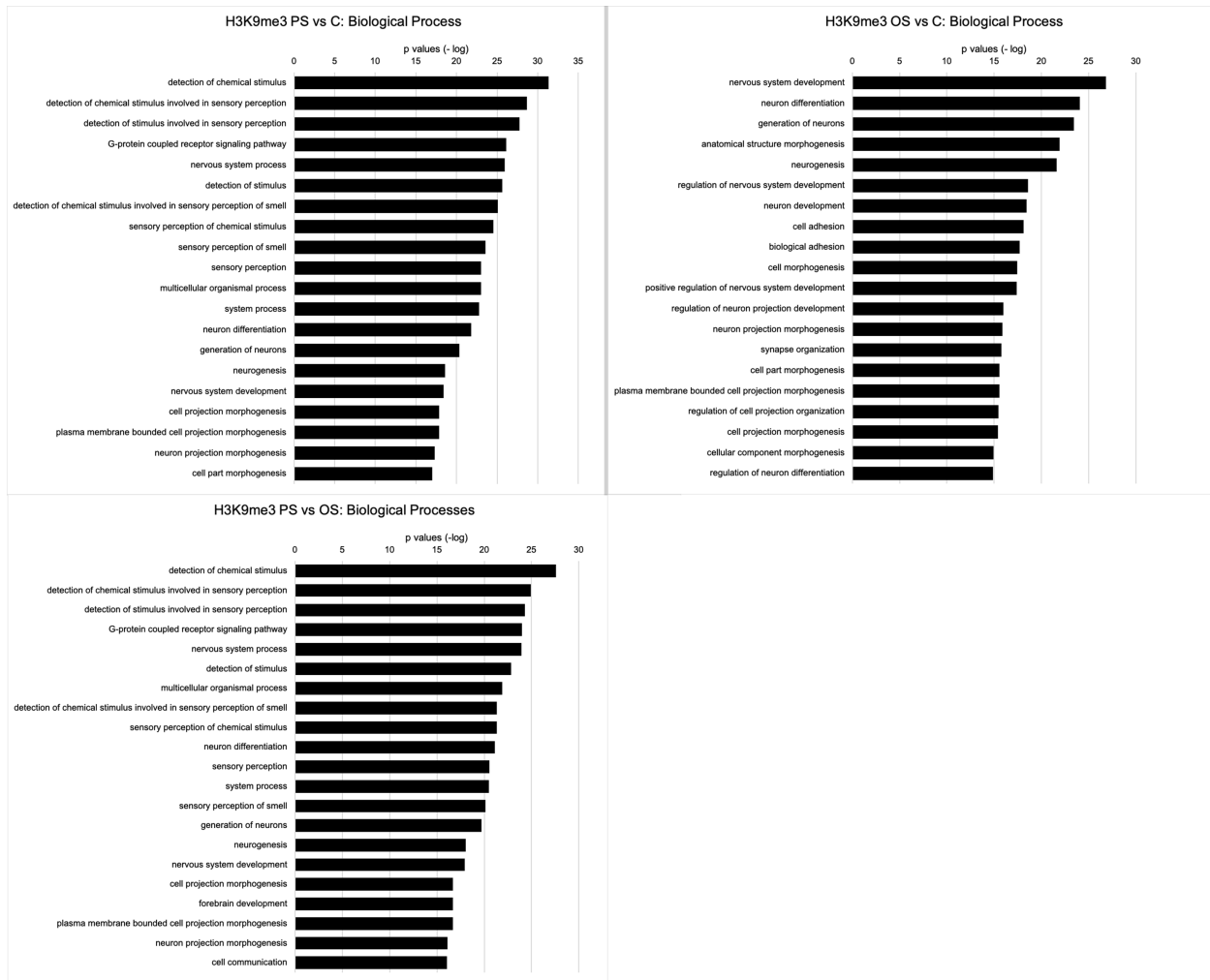
Figure 3.12: Gene Ontology: Biological Processes. H3K9me3

P-values of top 20 enrichment terms for PS vs C, OS vs C, and PS vs OS.
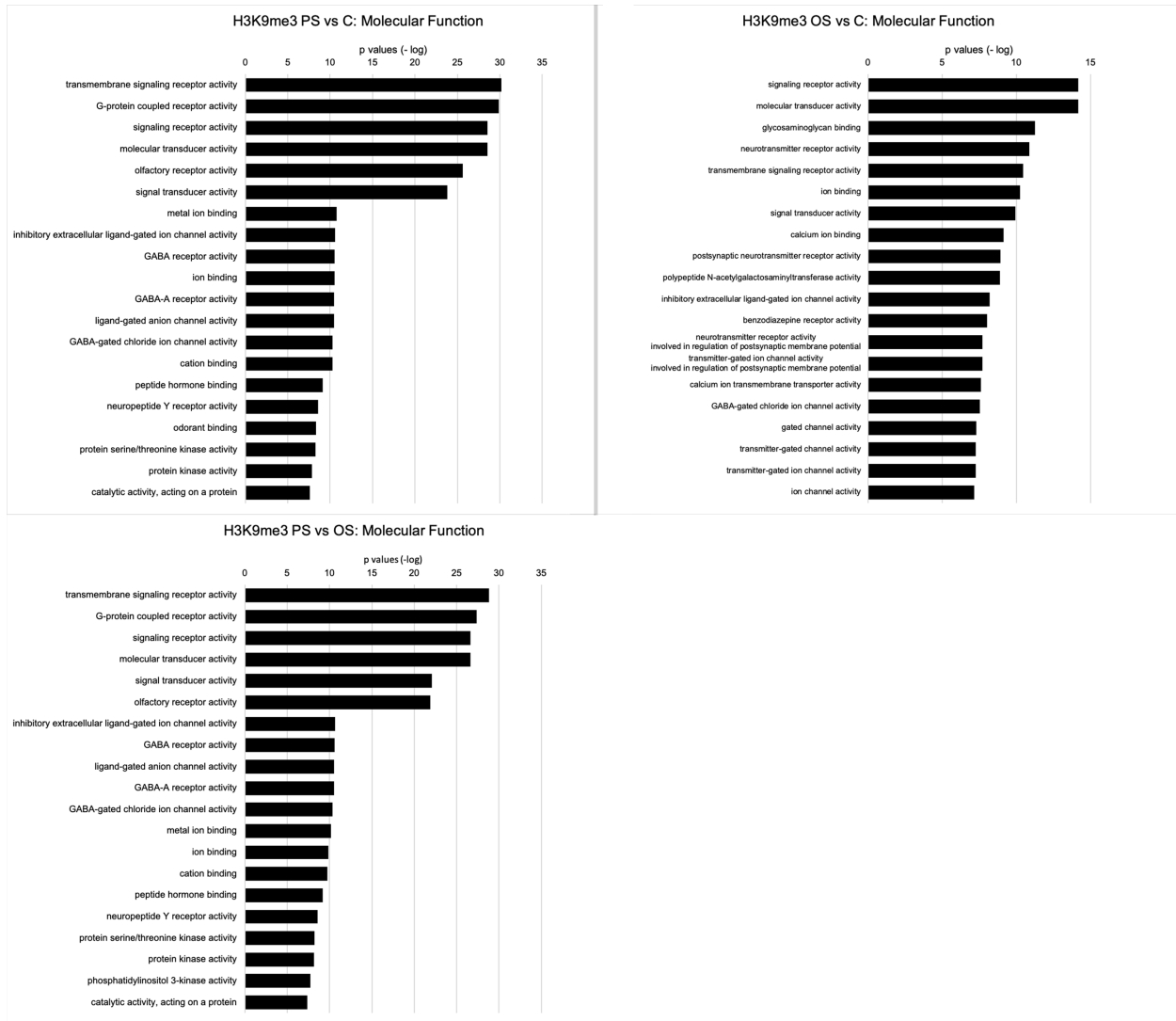
Figure 3.13: Gene Ontology: Molecular Function. H3K9me3

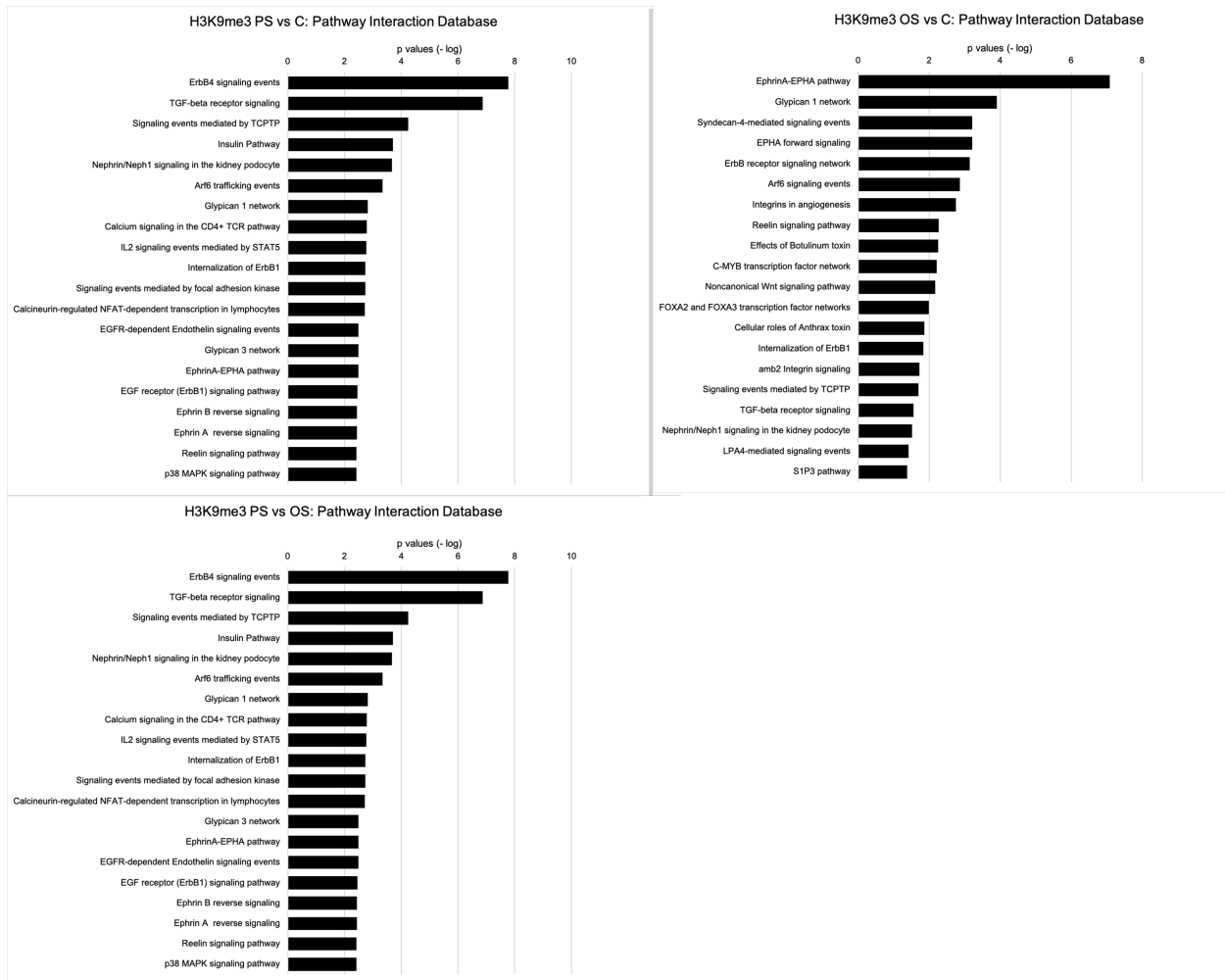P-values of top 20 enrichment terms for PS vs C, OS vs C, and PS vs OS.

Figure 3.14: Pathway Interaction Database. H3K9me3
P-values of top 20 enrichment terms for PS vs C, OS vs C, and PS vs OS.

3.6 Gene Ontology and network analysis of PS genes

ClueGO (v2.5.8) [37] is a Cytoscape plug-in that can be used to visualize large clusters of genes in a functionally grouped network. Peaks obtained from Rosalind analysis from PS conditions only were uploaded to perform cluster analysis. Ontology sources, such as KEGG, Gene Ontology: Biological Process, GO: Molecular Function, GO: Immune System Process, and WikiPathways, were used to create a functionally organized GO/pathway term network. A variety of flexible restriction criteria allows for visualization of different levels of specificity. Enrichment/depletion tests based on hypergeometric distribution was used in ClueGO, along with Bonferroni step-down for correcting P-values.

Cohen's Kappa coefficient measures inter-rater agreement for categorical terms. After the Kappa score is calculated between all the terms to form the edges, all items are iteratively compared and the

Table 3.3: ClueGO input statistics.

The number of peaks that were included in the downstream analysis.

Sample	Number of peaks	Number of peaks with >1.5 fold increase	% peaks used in analysis
ME2 PS vs OS	8659	3421	39.51
ME2 PS vs C	9170	3653	39.84
ME3 PS vs OS	49044	27428	55.93
ME3 PS vs C	49782	27164	54.57

functional groups defined. The Kappa score level can be adjusted from 0 to 1 to restrict the network connectivity. The default score of 0.4 was selected.

Due to the large number of peaks obtained from ChIP-seq computation pipeline, some p-values are small due to chance [38]. Bonferroni step-down procedure was used to correct for multiple testing, and a corrected p-value <0.01 was selected. Some peaks were unannotated and thus removed. As the gene list of peaks regions produced from the Rosalind include all peaks, peaks with at least a 1.5-fold increase from the minimum peak height was selected. (Table 3.3).

Pathway network visualization ClueGO allows for the visualization of pathways implicated from the genes obtained in ChIP-seq. Only PS genes were selected, and pathways with p-value <0.05 were used. P-values were corrected with Bonferroni step down. Network databases used included: KEGG, Reactome, and Wikipathways. Network specificity was global so as to provide a complete understanding of all the pathways implicated. Due to the limited number of peaks involved in OS conditions, the focus was placed on PS conditions.

H3K9me2: PS only From Figure 3.15, pathways implicated included: signal transduction, PI3K/Akt signaling pathway, signaling by receptor tyrosine kinases (RTK). Other categories of interest include: GPCR ligand binding and cellular responses to external stimuli.

As previously mentioned, signaling by RTK and GPCR has been implicated in shear stress and atherosclerosis. PI3K-Akt signaling pathway is pivotal in the involvement of cell survival and metabolism. Garcia-Cardena et. al has shown that HUVECs exposed to laminar shear stress results in the stimulation of the PI3K pathway and results in phosphorylation and activation of Akt [39]. It is also necessary for endothelial functions, such as NO synthase phosphorylation, for the promotion of HUVEC survival [40], [41]. Such results show that H3K9me2 is involved in RTK and PI3K-Akt signaling pathway, which contributes to the atheroprotective phenotype of PS.

H3K9me3: PS only From Figure 3.16, pathways implicated included: signal transduction, GPCR

downstream signaling, signaling by receptor tyrosine kinases (RTK). Other categories of interest include: cellular responses to external stimuli, specifically to stress. Similarly, such results show that H3K9me3 is involved in GPCR and RTK pathways, which contributes to the atheroprotective phenotype of PS.

Roscigilone et. al [42] showed that cellular depletion of $G\alpha_s$ delays lysosomal degradation of GPCRs through the disruption of GPCRs into the intraluminal vesicles of multivesicular bodies, thus revealing the role of $G\alpha_s$ in GPCR signaling and trafficking pathways.

Figure 3.15: ClueGO network: H3K9me2, global network specificity
The node size shows the term significance: the larger the term, the more significant it is.
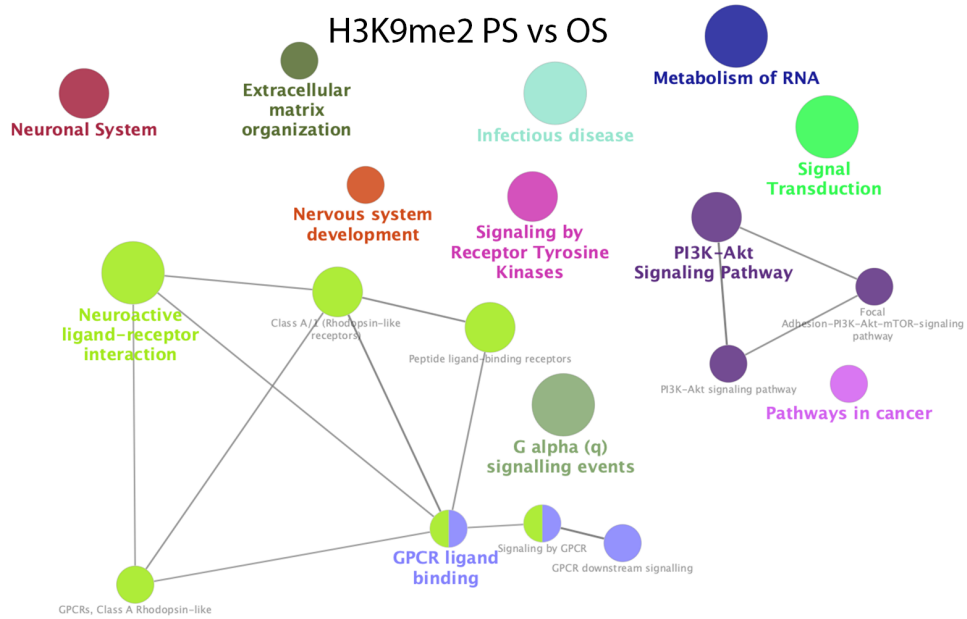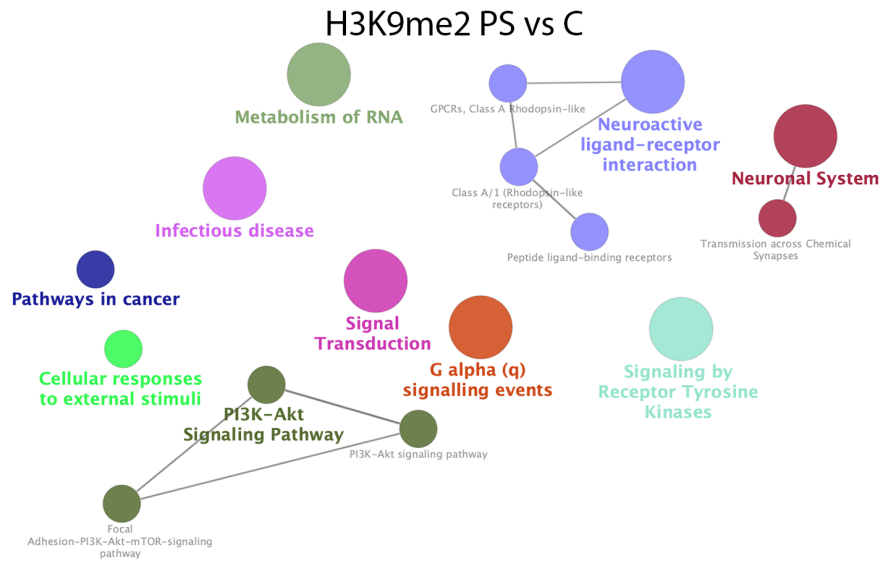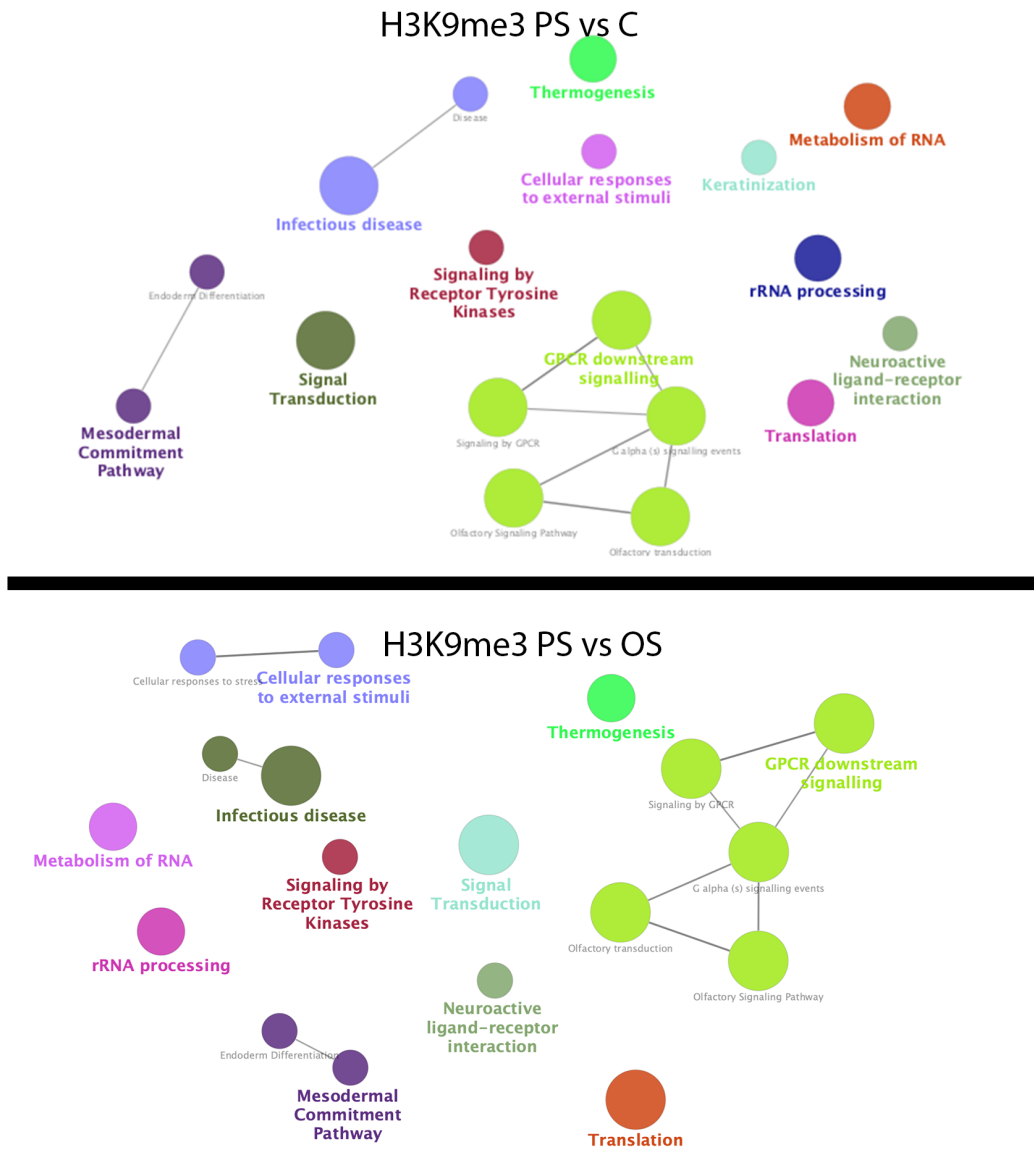
Figure 3.16: ClueGO network: H3K9me3, global network specificity
The node size shows the term significance: the larger the term, the more significant it is.

A deeper understanding of the involved categories and the associated genes allows us to identify and confirm various players involved in different pathways associated with atheroprotective PS phenotype from literature search. Here, the following categories of interest were selected:

Cell adhesion category included genes such as canonical genes such as E-selectin (SELE), P-selectin (SELP), VCAM-1 [43]. SELE is found on ECs that are stimulated by inflammatory cytokines such as tumor necrosis factor (TNF)-α, interleukin (IL)-1α, or platelet factor 4 (PF4), which is a platelet-specific chemokine that is released on platelet activation. Other phosphoinositide-3-kinase (PI3K) genes, aside from its role as seen in Figure 1.2, such as PIK3CB, PIK3CG, PIK3R1, are involved also in immune response. Serine/threonin protein kinase B (Akt) regulates cellular functions such as cell growth, proliferation, adhesion, and cell death through phosphorylation to activate or suppress the associated proteins [44]. A study conducted by Tsoyi et al. [45] shows that a negative regulator of the PI3K/Akt pathway can significantly prevent monocyte adhesion to TNF-α-induced ECs through VCAM-1 regulation.

Cell population proliferation is a key contributor to plaque growth, and progression through cell cycle requires activation of cyclin-dependent protein kinase (CDK) and a regulatory subunit named cyclin. CDK inhibitory proteins (CKIs) interact with and inhibit the activity of CDK/cyclins. Cell migration occurs at the G1/S phase of the cell cycle, and CDKs and CKIs are among the studied mechanisms that regulate events that control cell proliferation and migration [46]. Some genes of interest include CDK6, CDKN2B, retinoblastoma transcriptional corepressor 1(RB1). Laminar shear stress inhibits the activity of the retinoblastoma protein (pRb)-CDK system, thus inhibiting cell proliferation that leads to atherosclerosis [47].

Sensory perception, which includes response to stimulus, detection of stimulus, and cellular response to endogenous stimulus, involves genes such as Piezo2, PIK3CG. While not much is known about the context of Piezo2 in ECs in the detection of shear stress [48], Piezo proteins have been characterized as mechanosensitive ion channels that sense a wide range of repetitive mechanical stimuli and are modulated by local changes in resting membrane tension and activity of G protein-coupled pathways [49]. Piezo2 knockdown is also shown to inhibit HUVEC proliferation and migration *in vitro* [50].

G protein-coupled receptor activity and transmembrane signaling receptor activity were also categories of interest, thus confirming the results from the Pathway Interaction Database (Section 3.5).

These results show us that some canonical genes, such as SELE, VCAM-1, PI3K, that are implicated in multiple essential endothelial cell functions, is stimulated in response to PS. Other categories also provide insight into the mechanism of mechanotransduction of external stimuli (PS) into the nucleus for H3K9me2 and H3K9me3 expression.

Together, gene ontology analysis and network visualization show that H3K9me2 and H3K9me3

promotes activation of various pathways that are associated with cell survival, proliferation, adhesion and inflammation. These pathways have been implicated in the progression of atherosclerosis, thus providing insight into the mechanism and atheroprotective nature of PS on HUVECs.

3.7 Known and *de novo* enriched motifs in ChIP-seq peaks

Analyzing the DNA sequences underlying peak regions provides insights into the DNA binding preferences of the H3K9me2 and H3K9me3. These various motifs show motifs that are enriched in peaks from H3K9me2/me3 ChIP-seq data. Some of the motifs are found involved in pathways obtained from gene ontologies and pathway interactions, such as PI3K/Akt signaling. However, H3K9me2/me3 are recognized as repressive marks within gene-poor regions. As such, great care must be taken before hypothesizing if there is a direct suppressing effect from methylating H3K9 in these genes.

3.7.1 Known motifs

A strategy in motif analysis is to scan the peak regions for defined motifs. Motifs are derived from various *in vitro* or *in vivo* experiments and are found in public databases. Figure 3.17 shows the top five known motifs found for H3K9me2 and H3K9me3 PS vs OS and PS vs C conditions, respectively.

H3K9me2 PS vs C The top two motifs are found to be BAPX1 (19.99%) and BARX1 (14.43%). Transcriptional repressor BAPX1 (also known as Nkx3.2) is found to be inhibited by H3K9 deacetylation, thus contributing to SIRT6-mediated BAPX1/GATA5 signal transduction pathways in the regulation of endothelial function, such as protection against endothelial injury like hypertension [51]. Literature search does not show relation of BARX1 to endothelial cell-related functions, since it suggests a biased expression in stomach (https://www.ncbi.nlm.nih.gov/gene/56033).

H3K9me2 PS vs OS The top two motifs are found to be FOXO3 (17.82%) and BARX1 (14.45%). FOXO3 is involved in induction of cell cycle arrest and oxidative stress-induced apoptosis in HUVECs. As previously mentioned, PI3K/Akt signaling is necessary for cell survival and growth and is mediated by the phosphorylation of FOXO proteins by Akt [52], [53], [54]. Similar to H3K9me2 PS vs C, literature search does not show relation of BARX1 to endothelial cell-related functions, since it suggests a biased expression in stomach (https://www.ncbi.nlm.nih.gov/gene/56033).

H3K9me3 PS vs C The top two motifs are found to be GATA3 (28.17%) and GATA6 (15.95%), both of which are expressed preferentially in HUVEC. On a functional level, GATA3 knockdown inhibits angiopoietin (Ang)-1 AKT signalling, which is associated with cell migration, and survival. It is also shown to mediate anti-inflammatory effect of Ang-1-Tie2 through attenuation of VCAM-1 expression in cultured

human primary endothelial cells [55], [56]. GATA6 is also involved in the angiogenic function (such as proliferation and migration) and survival of endothelial cells, and acts as a positive regulator of VCAM-1 gene transcription [56], [57]. VCAM-1 peaks were found in intergenic and intron regions, and is involved in inflammation.

H3K9me3 PS vs OS The top two motifs are found to be MEF2B (21.3%) and BARX1 (13.61%). Literature search does not show relation of these motifs to endothelial cell-related functions. MEF2B is involved in B-cell studies (https://www.ncbi.nlm.nih.gov/gene/100271849). Similarly to H3K9me2 PS vs OS and PS vs C, literature search does not show relation of BARX1 to endothelial cell-related functions, since it suggests a biased expression in stomach (https://www.ncbi.nlm.nih.gov/gene/56033).

3.7.2 *De novo* motifs

Another strategy is to search for sequences in peak regions without any *a priori* assumptions. HOMER looks for motifs with differential enrichment between two set of sequences, which are the target sequences of interest and a set of background sequences. The background sequences are selected by default parameters. Compared to known motifs which only provide information about knows motifs from various databases, de novo motifs allows for the direct query of sequences to discover which motifs are most enriched.

Compared to known motifs, *de novo* motifs show up in less than 3% of the peaks in all cases (Figure 3.18). Here, the following motifs mentioned are those related to literature search involving expression in endothelial cells only.

H3K9me2 PS vs C

Known Motif Enrichment Results

	Match	% peaks with motif (% background) ↓	p-Value
	Bapx1(Homeobox)	19.99% (18.46%)	0.00010
	Barx1(Homeobox)	14.43% (13.13%)	0.00100
	STAT6(Stat)	8.17% (6.69%)	1.00e-7
	THRa(NR)	1.40% (0.99%)	0.00010
	LXRE(NR),DR4	0.55% (0.30%)	0.00010

H3K9me2 PS vs OS

Known Motif Enrichment Results

	Match	% peaks with motif (% background) ↓	p-Value
	Foxo3(Forkhead)	17.82% (16.36%)	0.00100
	Barx1(Homeobox)	14.45% (12.97%)	0.00010
	STAT6(Stat)	8.11% (6.62%)	1.00e-7
	MafF(bZIP)	5.88% (4.94%)	0.00010
	LXRE(NR),DR4	0.55% (0.32%)	0.00100

H3K9me3 PS vs C

Known Motif Enrichment Results

	Match	% peaks with motif (% background) ↓	p-Value
	GATA3(Zf)	28.17% (26.84%)	1.00e-10
	Gata6(Zf)	15.95% (14.88%)	1.00e-10
	KLF3(Zf)	0.56% (0.37%)	1.00e-10
	LXRE(NR),DR4	0.52% (0.32%)	10.00e-12
	Sp1(Zf)	0.13% (0.05%)	1.00e-10

H3K9me3 PS vs OS

Known Motif Enrichment Results

	Match	% peaks with motif (% background) ↓	p-Value
	Mef2b(MADS)	21.38% (20.36%)	1.00e-7
	Barx1(Homeobox)	13.61% (12.68%)	1.00e-9
	Brn2(POU,Homeobox)	3.54% (3.08%)	1.00e-8
	KLF14(Zf)	2.20% (1.86%)	1.00e-7
	Sp1(Zf)	0.14% (0.05%)	1.00e-10

Figure 3.17: Top 5 known motifs: H3K9me2 and H3K9me3 PS conditions. Conditions include PS vs OS and PS vs C. Sorted in descending order of % peaks with motifs.

H3K9me2 PS vs C

de novo Motifs

de novo Motifs	Match	% peaks with motif (% background) ↓	p-Value
TCACAGAGTTGA	VDR(NR),DR3	0.55% (0.01%)	1.00e-84
TATGTGAAGATA	FOXB1	0.54% (0.00%)	1.00e-97
CACACATCACAA	PH0134.1_Pbx1	0.52% (0.00%)	1.00e-92
GATTCTACAAAA	STAT6(Stat)	0.48% (0.01%)	1.00e-62
TTCAAAACTGCT	LIN54	0.47% (0.00%)	1.00e-80

H3K9me2 PS vs OS

de novo Motifs

de novo Motifs	Match	% peaks with motif (% background) ↓	p-Value
TGCAGATTCTAC	PRDM9(Zf)	0.62% (0.01%)	1.00e-91
GAAGATATTTCC	ZNF528(Zf)	0.61% (0.01%)	1.00e-89
TTCAACTCTGTG	POL009.1_DCE_S_II	0.56% (0.01%)	10.00e-67
GCACACATCACG	PB0208.1_Zscan4_2	0.55% (0.00%)	1.00e-93
AGAATGCTTCTG	POL008.1_DCE_S_I	0.53% (0.01%)	10.00e-68

H3K9me3 PS vs C

de novo Motifs

de novo Motifs	Match	% peaks with motif (% background) ↓	p-Value
CCCGCCTCAGCC	SP2	2.26% (1.05%)	1.00e-116
CCCGGCTAAT	PH0032.1_Evx2	1.60% (0.56%)	1.00e-140
TAGTAGAGACGG	PRDM14(Zf)	1.17% (0.38%)	1.00e-115
TGGCGGGCGCCT	HES7	1.13% (0.34%)	1.00e-126
GAATGCTTCTGT	PB0050.1_Osr1_1	0.18% (0.00%)	1.00e-134

H3K9me3 PS vs OS

de novo Motifs

de novo Motifs	Match	% peaks with motif (% background) ↓	p-Value
GTAGCTGGGACT	NHLH1	1.23% (0.34%)	1.00e-150
TAGAATCTGCAA	PB0125.1_Gata3_2	0.20% (0.01%)	10.00e-126
TCACAAAGAAGT	SOX10	0.20% (0.00%)	1.00e-123
TCAACTCTGTCA	MEIS2	0.19% (0.01%)	1.00e-122
ATGTGAAGATAT	GATA3(Zf),DR4	0.19% (0.01%)	1.00e-115

Figure 3.18: Top 5 *de novo* motifs: H3K9me2 and H3K9me3 PS conditions. Conditions include PS vs OS and PS vs C. Sorted in descending order of % peaks with motifs.

3.8 Integration of ChIP-seq data with RNA-seq data

Studies over the past several decades have elucidated different mechanisms of atherosclerosis, such as endothelial dysfunction, chronic inflammation, lipid deposition. A deeper understanding of molecular and biological functions of roles different genes play in can be used to further understand the relationship between various epigenetic modifications.

Prior studies that make use of RNA-seq [10] has implicated differentially expressed genes (log2 fold change) that were upregulated or downregulated in PS or OS conditions. Briefly, RNA-seq is used to quantify gene expressions, while ChIP-seq is used to chart the genomic landscape of histone modifications [58].

This analysis has been taken further to compare with H3K9me2 and H3K9me3 ChIP-seq peaks. All peaks from the computation pipeline was used in this comparison. Figure 3.19 shows the overlap of genes that were differentially expressed (DE) from RNA-seq downstream analysis and ChIP-seq peaks in H3K9me2 and H3K9me3.

The genes in RNA-seq are upregulated or downregulated in PS when compared to OS (Table 3.4). From prior RNA-seq experiments, 30 genes in total were defined as significantly differentially expressed [10]. 11 genes had a negative OS vs PS log2 fold change, meaning that genes in OS conditions were downregulated relative to PS. 19 genes had a positive OS vs PS log2 fold change, meaning that genes in OS conditions were upregulated relative to PS, which we assume to mean that these genes are upregulated in PS conditions.

After comparison of H3K9me2 ChIP-seq peaks with DE RNA-seq genes, genes 1 out of 11 genes are upregulated in PS (KLF4). 3 out of 19 genes were downregulated in PS (CCNA1, CXCR4, RARB). From the RNA-seq experiments in H3K9me3, 4 out of 11 genes are upregulated in PS (EPAS1, KLF4, LINC00520, RXRA). 7 out of 19 genes were downregulated in PS (CCNA1, CCNA2, CCNE2, CXCR4, HAT1, HIF1A, RARB).

Since H3K9me2 ChIP-seq and RNA-seq downstream results did not produce sufficient insight into the atheroprotective phenotype, H3K9me3 was chosen as the focus of understanding the histone modifications induced by shear stress.

Since H3K9 methylations are related to silenced transcription, the genes produced from the computational pipeline are assumed to be repressed. Downregulation of such genes show the repressive effect H3K9me3 has on these genes. However, there are several questions and challenges to translating such mechanobiological studies to creating a comprehensive understanding of the network and pathway of genes involved. For example, the potential interaction network regulates the expression of important genes involved in proliferation, oxidative stress, inflammation, and migration. While the following are delineated into specific categories,
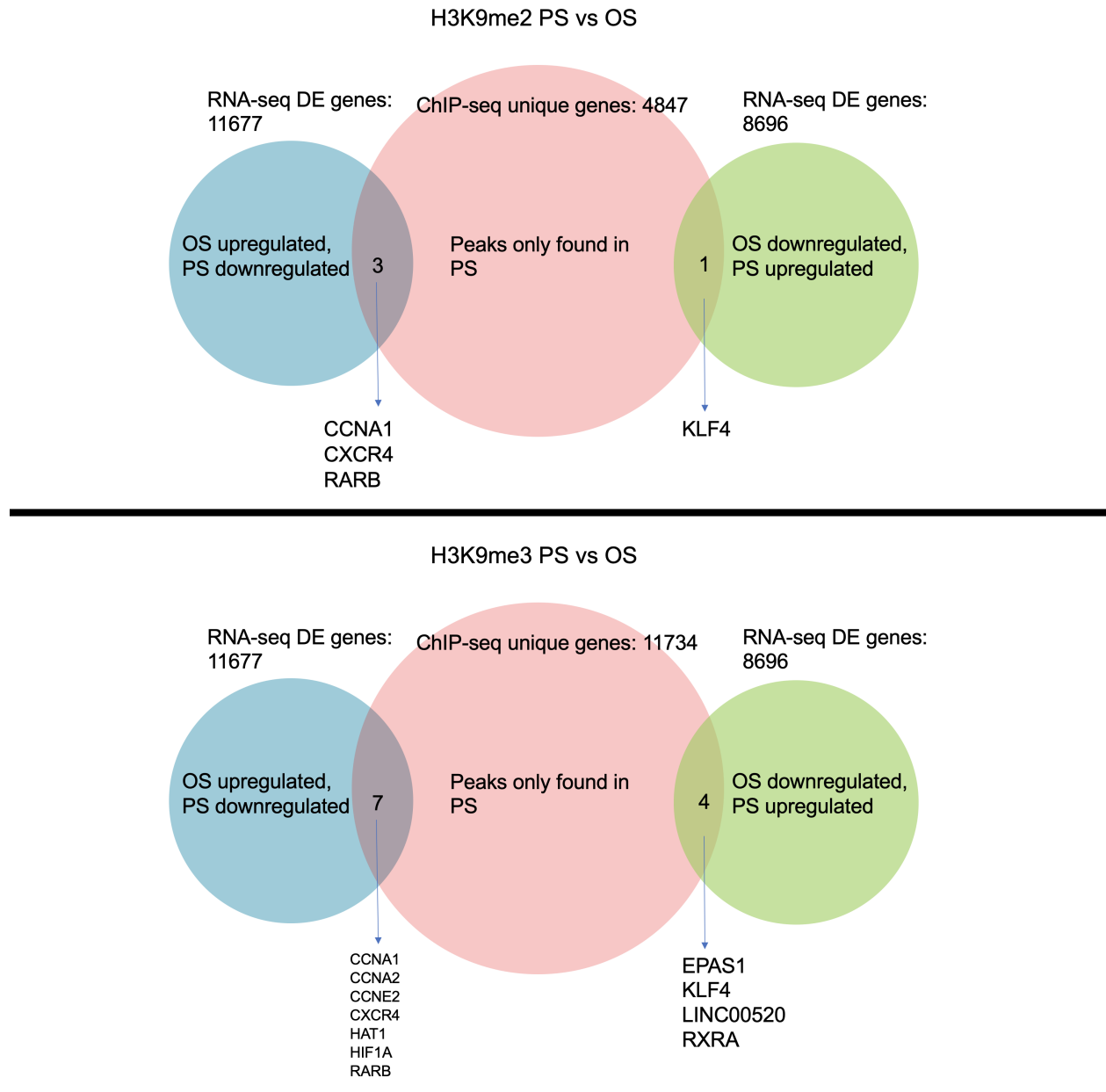
Figure 3.19: ChIP-seq and RNA-seq analysis
Overlap of differentially expressed (De) genes from RNA-seq and peaks from ChIP-seq. ChIP-seq peaks were obtained from Rosalind ChIP-seq analysis pipeline. RNA-seq data was obtained from prior study conducted [10]. Top: H3K9me2, bottom: H3K9me3

Table 3.4: Directionality of RNA-seq Log2 fold change values.

Positive values (green) mean that OS is upregulated with respect to PS. Negative values (blue) mean that OS is downregulated with respect to PS.

	Gene Name	Log2 Fold Change (OS vs PS)
H3K9me2	CXCR4	2.31
	RARB	0.30
	CCNA1	0.55
H3K9me2	KLF4	-2.42
H3K9me3	CCNE2	0.70
	CCNA1	0.55
	CCNA2	0.32
	CXCR4	2.31
	HAT1	0.51
	RARB	0.30
	HIF1A	0.26
H3K9me3	KLF4	-2.42
	LINC00520	-1.93
	RXRA	-0.66
	EPAS1	-0.78

these genes may also be involved in multiple overlapping categories.

Proliferation ECs remain in a quiescent and non-proliferative under normal conditions. Laminar shear stress inhibits EC proliferation. If the endothelial monolayer sustains an injury, a rapid burst of proliferation occurs through cell-cell contact. Cell cycle progression is controlled by periodic activation of CDKs (Section 3.6).

Cyclin A protein is preferentially expressed in proliferating ECs [59]. YAP pathway regulates cell proliferation, differentiation, and tissue regulation [60]. Under atheroprotective flow patterns, YAP activity is decreased and cell cycle gene cyclin A expression is found to be downregulated [61]. Cyclin A2 (CCNA2) is involved in the initiation of mitotic chromatin condensation in the cell cycle [62]. In the mitochondria, histone acetyltransferase (HAT1) is involved in adenosine monophosphate (AMP)–activated protein kinase (AMPK) and creates a more relaxed chromatin-DNA structure that favours transcription [63].

Downregulation of these genes shows the atheroprotective effects of H3K9me3 from PS on repressing proliferation-association genes.

Oxidative stress Through the upregulation of vascular endothelial growth factor (VEGF), nitric oxide (NO) and reactive oxygen species (ROS) under hypoxic conditions, HIF1 is able to cause EC dysfunction, proliferation, and inflammation, thus contributing to the progression of atherosclerosis [64]. Downregulation of HIF1 shows the atheroprotective effect H3K9me3 has on atherosclerosis. On the other hand, EPAS1

45

is upregulated despite repression-associated H3K9me3. EPAS1, or HIF2A, is an important regulator of hypoxia response. Accumulation of cells in plaque with decreased oxygen tension leads to an increased oxygen demand inside the plaque. Hypoxia thus correlates with plaque severity. HIF1A and HIF2A may play opposing roles in cellular processes. Ablation of HIF2A function in murine vascular ECs display defects in vessel integrity and tumor angiogenesis [65]. In vascular ECs, HIF2A regulates the expression of VEGF, VEGF-associated receptors, and Tie2. Stavik et. al [9] has shown that hypoxia reduces the expression of pro-thrombotic tissue factor pathway inhibitor (TFPI) in ECs through a reduced expression of HIF2A and is possibly intertwined with HIF1A pathways, and results in enhanced endothelial procoagulant activity which mediates the severity of plaque formation.

Migration Invasion into and migration through the extracellular matrix is necessary for ECs to assemble a vascular system. Molina et. al [66] showed that activation of chemokine receptor CXCR4 by its ligand SDF-1 is shown to cause migration in in HUVECs. However, surface expression of CXCR4 was shown to be heterogenous amongst ECs. Döring et. al [67] showed that vascular CXCR4 limits atheroclerosis by maintaining arterial integrity. They showed that deletion of the CXCR4 in arterial endothelial cells increase atherosclerotic lesion formation in hyperlipidemic mice, increases vascular permeability through WNT/β-catenin, and sustains VE-cadherin that controls permeability. Laminar shear stress has been shown to inhibit CXCR4 [68], which is also involved in apoptosis. CXCR4 overexpression induces apoptosis and inhibits laminar shear stress anti-apoptotic action.

Inflammation Kruppel-like factor 4 (KLF4) is an important anti-inflammatory atherprotective transcription factor that is supressed in disturbed flow. KLF4 is found to be upregulated under PS conditions and inhibits VCAM-1 induction and eNOS production, which is central to endothelial homeostasis and vascular function. Overexpression of KLF4 is found to be protective against atherosclerosis and thrombosis [69], thus contributing to the atheroprotective phenotype of PS. Interestingly, KLF4 is still upregulated despite H3K9me3 and its associated repression. LINC00520, or C14orf34, a long-non-coding RNA, is also shown to correlate highly with that of eNOS under PS conditions as compared with OS [70]. Retinoid X receptor alpha (RXRA) is known to function as one of the primary receptors of retinonic acid, and activation of retinonic acid signaling has been shown to repair damaged tight junction barriers and promote endothelial functions in through boosting eNOS activity and nitric oxide production[71]. Canonical genes like VCAM-1 and SELE were found to be upregulated in H3K9me3 PS conditions, when compared with OS and control. ICAM-1 was not found to be significantly up-regulated, and this may be VCAM-1 is shown to play a more important role in early atherosclerosis than ICAM-1 [72]. However, such genes were not significantly upregulated in H3K9me2 conditions.

3.9   H3K9me3 is expressed in nucleus of ECs in mild but not severe atherosclerosis

Next, we would like to observe the location of expression of H3K9me3 in human samples. Transverse sections of coronary artery with mild and severe lesions were stained to identify presence of H3K9me3 in endothelial cells. Samples with severe lesions were taken from patients who suffered from chronic kidney disease (CKD) and have undergone hemodialysis. Immunostaining (Figure 3.20) of of mild lesions of endothelial cells in human coronary arteries show overlap of H3K9me3 signals in areas which exhibit DAPI staining, suggesting that H3K9me3 modifications occurs in chromatin regions in mild atherosclerosis. However, such overlap are not observed in severe lesions, suggesting that H3K9me3 does not occur in advanced stages of atherosclerosis, and thus would not be able to repress downstream processes that regulate atheroprotection. Bioinformatics analysis has also implicated chronic kidney disease and dialysis-related mortality from GWAS catalog (Figure 3.21).
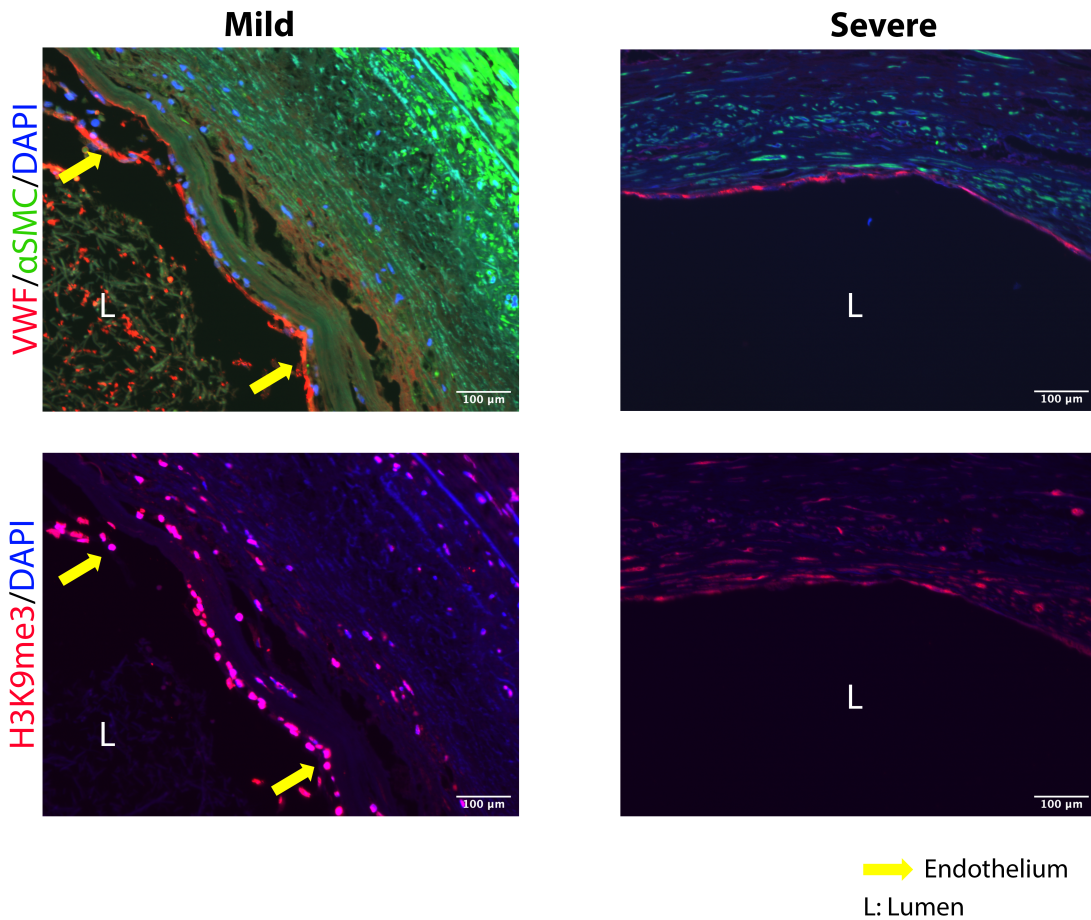
Figure 3.20: Immunostaining results
Samples are 4-μm thick sections of human coronary artery. Left: mild lesions. Right: severe lesions. Top: Staining for VWF (red), α-SMA (green), and DAPI (blue). Bottom: Staining for H3K9me3 (red) and DAPI (blue). Magnification: 10x. Arrows indicate layer of endothelial cells. L: lumen.
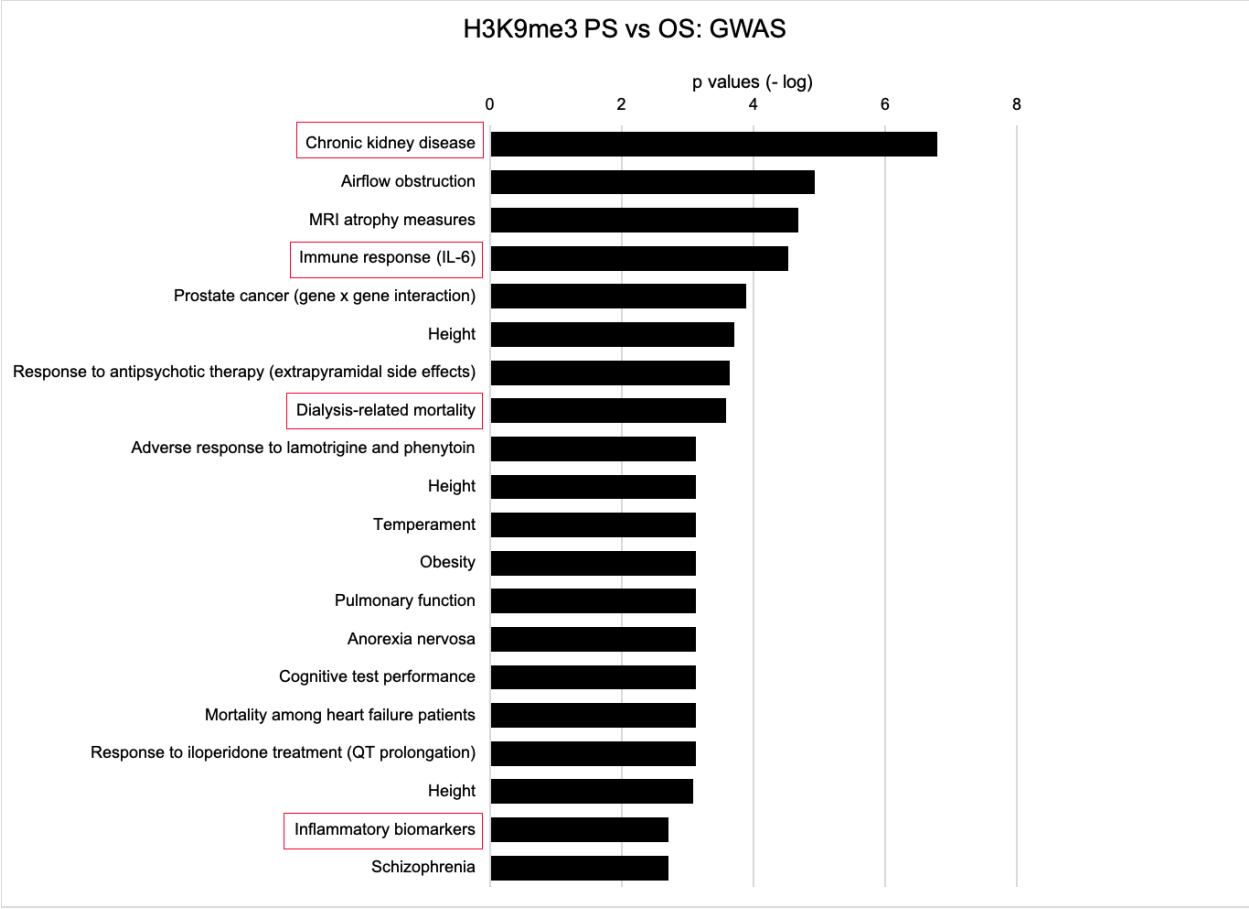
Figure 3.21: GWAS catalog. Ontologies in H3K9me3.
P-values of top 20 enrichment terms for H3K9me3 PS vs OS. Rectangles indicate categories of interest.

4 Conclusion, Discussion, and Future Directions

Latest advances in the vascular mechanobiology field is the discovery of key regulators that control a large network of genes. Such discovery is important since these regulators may be therapeutic targets for the treatment and prevention of atherosclerosis. Therefore, key regulators of global transcription and translation are of interest in this study, as they alter genomic DNA in order to control accessibility of DNA sequences. In particular, this study focuses on the biological and molecular functions of histone modifications such as H3K9 methylation under shear stress.

Hemodynamic forces are seen to affect histone modification in ECs from *in vitro* and *in vivo*. PS leads to H3K9 methylation which leads to various signaling pathways and gene expression to suppress atheroprone phenotypes, such as inflammation, migration, and proliferation. On the other hand, OS leads to atheroprone phenotypes, thus contributing to atherosclerosis. Once shear stress is applied to the cell, various intracellular pathways are triggered. Such mechanostransduction pathways converge on common signaling pathways, such as GPCRs and PI3K pathways, as seen in the top 20 Pathway Interaction Database.

The question of how epigenetic modifications, in particular H3K9 methylation, contribute to the atheroprotective phenotype of PS induced in ECs is still unresolved. Here, we investigate H3K9me2 and me3 in cultured HUVEC after 24 hours of exposure to PS and OS. Bioinformatics analysis reveals categorization of genes related to various representative biological processes and molecular functions under H3K9 methylation in response to shear stress. Some categories and associated genes of interest include inflammation, migration, proliferation, and oxidative stress. Other categories also include pathways that are involved in the detection of various sensory stimulus and can provide us with insight to the transmission of mechanical forces into the nucleus, thus allowing us to understand the interplay between external mechanical stresses on epigenetic modifications. Future experiments, such as qRT-PCR, can be conducted to independently verify any increase of expression in select genes of interest found in these ontologies.

This thesis has taken the first step in establishing that atheroprotective PS induces H3K9me2 and me3 in HUVECs. Through bioinformatics analysis, various signaling pathways that are shown to be involved in biological cellular functions to maintain vascular homeostasis are implicated by the repressive function of H3K9me2 and me3 marks. Some of these pathways include GPCR, PI3K/Ak and MAPK, while others involve the mechanotransduction of signals to the nucleus, where H3K9me2/me3 takes place.

While alterations in the transcriptional genome has been studied, DNA hypermethylation is one of the main epigenomic features that has been associated with atherosclerosis. Studies have shown that there is a positive correlation between the levels of global DNA hypermethylation of cytosines at CpG-regions of region and progression of atherosclerotic lesion [73], [74]. However, the effect of histone modifications

on the development and progression of atherosclerosis have not been as extensively studied. Illi et. al [75] showed that shear stress induced H3S10 phosphorylation and H3K14 acetylation. Bondareva et. al [76] elucidated the mechanism that links OS to EC phenotype through studying H3K27ac, which is associated with active transcription. They then showed that regulatory elements were overrepresented in several signaling pathways, including MAPK, PI3K/Akt, WNT, NOTCH, HIPPO (YAP/TAZ), and investigated the associated transcription regulations through binding motifs. Thus, they have shown that H3K27ac is a key response to OS, and leads to the activation of multiple genes involved in downstream signaling pathways. Other studies on histone modifications in cardiovascular diseases, specifically H3K9, are usually limited to acetylation, or methylation expression in cells such as VSMC. A study conducted by Greisel [77] on analysis of H3K9 methylation in atherosclerotic plaques of patients with carotid artery stenosis did not show significant differences in the expression of histone methyltransferases (HMTs) associated with H3K9 methylation in ECs. This may be since methylation at lysine residues K9 lead to gene inactivation, and as such, there is low or no detectable expression of the responsible HMTs. Harman et. al [78] showed that reduced H3K9me2 in disease enhances binding of transcription factors at inflammation-responsive genes in VSMC.

The main difference with other histone modification studies is that H3K9 methylation is correlated with transcriptional repression. 90% of the peaks in from ChIP-seq for H3K9me2/me3 is found to be in intergenic regions and introns. What is the link between peaks in specific genomic region and the enrichment of the regulatory histone marks? Exploratory work into such a question can aid be helpful in mapping out the epigenetic mechanisms involved in atherosclerosis.

Comparisons of genes only found in PS with other conditions (PS vs OS, PS vs C) showed that there were no significant changes across. Instead, more differences occur within H3K9me2 and H3K9me3. A comparison of biological processes involved in H3K9me2 and H3K9me3 revealed that H3K9me2 was implicated in nervous system-related ontologies. This may also be due to the relatively low number of H3K9me2 PS peaks (around 10000) compared to H3K9me3 peaks (around 50000). The ratio of PS to OS and PS to C peaks for H3K9me2 is also larger than that of H3K9me3: around 12-fold of PS:OS and PS:C peaks, with around 1.15-fold for PS:OS and around 3.3-fold for PS:C. Downstream analysis also revealed limited results in the atheroprotective effects of shear stress on H3K9me2, which is the main reason for focusing on the effects PS has on H3K9me3. This is not to say that H3K9me2 does not play a role in atheroprotection, but rather the limitations in the sequencing data obtained.

When integrating RNA-seq data obtained from prior studies, an interesting thing to note what that KLF4 is still upregulated despite H3K9me3 silencing. Atheroprotective PS flow is shown to induce KLF4 to activate genes essential for EC homeostasis through acetylation of H3K27 [79]. This implies that 1) H3K9 methylation is not the only epigenetic regulation on a single gene that is involved in atheroprotective shear

stress and 2) there may be co-occurances of modifications on the same peptide, leading to a acetylation-methylation switch [80]. More work between the interplay of histone modifications can be conducted in order to reveal the network of epigenetic regulation of PS.

Studies have been shown that there is an association between CKD on hemodialysis and atherosclerosis [81]. CKD is characterized by systemic inflammation, which is also one of the main mechanisms of atherosclerosis. CKD patients have extensive coronary heart disease with higher proportion of calcified plaques, greater media thickness, and the presence of medial calcification. Plaque composition of such lesions evolved from necrotic core to calcium-rich plaques as renal functions decline [82]. Through bioinformatics analysis of H3K9me3 PS only conditions, genome-wide association studies (GWAS) shows that chronic kidney disease (PMID:20383146) is enriched, with 17 out of 18 genes found in this term. This shows that there is a connection as to why there is no signal of H3K9me3 expression in CKD patients with severe lesions that have gone through dialysis. An exploration into the epigenetic landscape of CKD patients can allow us to understand the progression of H3K9 methylation over the progression of disease. While cell culture allow us to associate various molecular functions and pathways through bioinformatics analysis, sustained insight through human samples allow us to track the progression of epigenetic modifications in a disease. As such, a future area of interest could be the progression of H3K9 methylation in association with CKD and atherosclerosis.

Finally, a major challenge is that endothelial phenotypes are highly heterogenous over different regions in the cardiovascular system. As such single cell experiments can compensate for the spatial and temporal profiling of genomic behavior under different shear stress patterns.

Despite various advances, much work is needed to determine the roles different shear stress patterns play on histone modifications and other epigenetic regulations play, and how these various modifications contribute the endothelial homeostasis to maintain an atheroprotective phenotype.

References

[1] J.-J. Chiu and S. Chien, "Effects of Disturbed Flow on Vascular Endothelium: Pathophysiological Basis and Clinical Perspectives", *Physiological Reviews*, vol. 91, no. 1, pp. 327–387, Jan. 2011.

[2] N. Niu, S. Xu, Y. Xu, P. J. Little, and Z.-G. Jin, "Targeting Mechanosensitive Transcription Factors in Atherosclerosis", *Trends in Pharmacological Sciences*, vol. 40, no. 4, pp. 253–266, Apr. 2019.

[3] Y.-S. J. Li, J. H. Haga, and S. Chien, "Molecular basis of the effects of shear stress on vascular endothelial cells", *Journal of Biomechanics*, vol. 38, no. 10, pp. 1949–1971, Oct. 2005.

[4] N. Baeyens, C. Bandyopadhyay, B. G. Coon, S. Yun, and M. A. Schwartz, "Endothelial fluid shear stress sensing in vascular health and disease", *Journal of Clinical Investigation*, vol. 126, no. 3, pp. 821–828, Mar. 2016.

[5] J. Zhou, Y.-S. Li, and S. Chien, "Shear Stress–Initiated Signaling and Its Regulation of Endothelial Function", *Arteriosclerosis, Thrombosis, and Vascular Biology*, vol. 34, no. 10, pp. 2191–2198, Oct. 2014.

[6] R. Ross, "Atherosclerosis — An Inflammatory Disease", *New England Journal of Medicine*, vol. 340, no. 2, F. H. Epstein, Ed., pp. 115–126, Jan. 1999.

[7] E. Falk, "Pathogenesis of Atherosclerosis", *Journal of the American College of Cardiology*, vol. 47, no. 8, pp. C7–C12, Apr. 2006.

[8] I. Tabas and A. H. Lichtman, "Monocyte-Macrophages and T Cells in Atherosclerosis", *Immunity*, vol. 47, no. 4, pp. 621–634, 2017.

[9] B. Stavik, S. Espada, X. Y. Cui, N. Iversen, S. Holm, M.-C. Mowinkel, B. Halvorsen, G. Skretting, and P. M. Sandset, "EPAS1/HIF-2 alpha-mediated downregulation of tissue factor pathway inhibitor leads to a pro-thrombotic potential in endothelial cells", *Biochimica et Biophysica Acta (BBA) - Molecular Basis of Disease*, vol. 1862, no. 4, pp. 670–678, Apr. 2016.

[10]   N. E. Ajami, S. Gupta, M. R. Maurya, P. Nguyen, J. Y.-S. Li, J. Y.-J. Shyy, Z. Chen, S. Chien, and S. Subramaniam, "Systems biology analysis of longitudinal functional response of endothelial cells to shear stress", *Proceedings of the National Academy of Sciences*, vol. 114, no. 41, pp. 10 990–10 995, Oct. 2017.

[11]   L.-H. Yeh, Y. J. Park, R. J. Hansalia, I. S. Ahmed, S. S. Deshpande, P. J. Goldschmidt-Clermont, K. Irani, and B. R. Alevriadou, "Shear-induced tyrosine phosphorylation in endothelial cells requires Rac1-dependent production of ROS", *American Journal of Physiology-Cell Physiology*, vol. 276, no. 4, pp. C838–C847, Apr. 1999.

[12]   Z. Chen, I.-C. Peng, X. Cui, Y.-S. Li, S. Chien, and J. Y.-J. Shyy, "Shear stress, SIRT1, and vascular homeostasis", *Proceedings of the National Academy of Sciences*, vol. 107, no. 22, pp. 10 268–10 273, Jun. 2010.

[13]   M. A. Gimbrone and G. García-Cardeña, "Endothelial Cell Dysfunction and the Pathobiology of Atherosclerosis", *Circulation Research*, vol. 118, no. 4, pp. 620–636, Feb. 2016.

[14]   H. Cedar and Y. Bergman, "Linking DNA methylation and histone modification: Patterns and paradigms", *Nature Reviews Genetics*, vol. 10, no. 5, pp. 295–304, May 2009.

[15]   K. Hyun, J. Jeon, K. Park, and J. Kim, "Writing, erasing and reading histone lysine methylations", *Experimental & Molecular Medicine*, vol. 49, no. 4, e324–e324, Apr. 2017.

[16]   J. S. Becker, D. Nicetto, and K. S. Zaret, "H3K9me3-Dependent Heterochromatin: Barrier to Cell Fate Changes", *Trends in Genetics*, vol. 32, no. 1, pp. 29–41, Jan. 2016.

[17]   B. Mifsud, K. Zarnack, and A. Bardet, *Practical guide to ChIP-seq: data analysis*, ser. Focus computational biology series. Boca Raton, Florida: CRC Press, 2019.

[18]   Y. Zhang, T. Liu, C. A. Meyer, J. Eeckhoute, D. S. Johnson, B. E. Bernstein, C. Nussbaum, R. M. Myers, M. Brown, W. Li, and X. S. Liu, "Model-based Analysis of ChIP-Seq (MACS)", *Genome Biology*, vol. 9, no. 9, R137, 2008.

[19] P. Khatri, M. Sirota, and A. J. Butte, "Ten Years of Pathway Analysis: Current Approaches and Outstanding Challenges", *PLoS Computational Biology*, vol. 8, no. 2, C. A. Ouzounis, Ed., e1002375, Feb. 2012.

[20] S. Bauer, "Gene-Category Analysis", in *The Gene Ontology Handbook*, C. Dessimoz and N. Škunca, Eds., vol. 1446, Series Title: Methods in Molecular Biology, New York, NY: Springer New York, 2017, pp. 175–188.

[21] H. Tipney and L. Hunter, "An introduction to effective use of enrichment analysis software", *Human Genomics*, vol. 4, no. 3, p. 202, 2010.

[22] Q. Li, J. B. Brown, H. Huang, and P. J. Bickel, "Measuring reproducibility of high-throughput experiments", *The Annals of Applied Statistics*, vol. 5, no. 3, pp. 1752–1779, Sep. 2011.

[23] Y. Chen, N. Negre, Q. Li, J. O. Mieczkowska, M. Slattery, T. Liu, Y. Zhang, T.-K. Kim, H. H. He, J. Zieba, Y. Ruan, P. J. Bickel, R. M. Myers, B. J. Wold, K. P. White, J. D. Lieb, and X. S. Liu, "Systematic evaluation of factors influencing ChIP-seq fidelity", *Nature Methods*, vol. 9, no. 6, pp. 609–614, Jun. 2012.

[24] Y. L. Jung, L. J. Luquette, J. W. Ho, F. Ferrari, M. Tolstorukov, A. Minoda, R. Issner, C. B. Epstein, G. H. Karpen, M. I. Kuroda, and P. J. Park, "Impact of sequencing depth in ChIP-seq experiments", *Nucleic Acids Research*, vol. 42, no. 9, e74–e74, May 2014.

[25] R. Nakato and K. Shirahige, "Sensitive and robust assessment of ChIP-seq read distribution using a strand-shift profile", *Bioinformatics*, vol. 34, no. 14, I. Birol, Ed., pp. 2356–2363, Jul. 2018.

[26] P. Kolasinska-Zwierz, T. Down, I. Latorre, T. Liu, X. S. Liu, and J. Ahringer, "Differential chromatin marking of introns and expressed exons by H3K36me3", *Nature Genetics*, vol. 41, no. 3, pp. 376–381, Mar. 2009.

[27] S. D. Funk, A. Yurdagul, P. Albert, J. G. Traylor, L. Jin, J. Chen, and A. W. Orr, "EphA2 Activation Promotes the Endothelial Cell Inflammatory Response: A Potential Role in Atherosclerosis", *Arteriosclerosis, Thrombosis, and Vascular Biology*, vol. 32, no. 3, pp. 686–695, Mar. 2012.

[28] S. D. Funk and A. W. Orr, "Ephs and ephrins resurface in inflammation, immunity, and atherosclerosis", *Pharmacological Research*, vol. 67, no. 1, pp. 42–52, Jan. 2013.

[29] H. Shakeri, A. B. Gevaert, D. M. Schrijvers, G. R. Y. De Meyer, G. W. De Keulenaer, P.-J. D. F. Guns, K. Lemmens, and V. F. Segers, "Neuregulin-1 attenuates stress-induced vascular senescence", *Cardiovascular Research*, vol. 114, no. 7, pp. 1041–1051, Jun. 2018.

[30] G. Xu, T. Watanabe, Y. Iso, S. Koba, T. Sakai, M. Nagashima, S. Arita, S. Hongo, H. Ota, Y. Kobayashi, A. Miyazaki, and T. Hirano, "Preventive Effects of Heregulin-β_1 on Macrophage Foam Cell Formation and Atherosclerosis", *Circulation Research*, vol. 105, no. 5, pp. 500–510, Aug. 2009.

[31] K. S. Russell, D. F. Stern, P. J. Polverini, and J. R. Bender, "Neuregulin activation of ErbB receptors in vascular endothelium leads to angiogenesis", *American Journal of Physiology-Heart and Circulatory Physiology*, vol. 277, no. 6, H2205–H2211, Dec. 1999.

[32] G. Siasos, D. Tousoulis, Z. Siasou, C. Stefanadis, and A. Papavassiliou, "Shear Stress, Protein Kinases and Atherosclerosis", *Current Medicinal Chemistry*, vol. 14, no. 14, pp. 1567–1572, Jun. 2007.

[33] S. Li, M. Kim, Y.-L. Hu, S. Jalali, D. D. Schlaepfer, T. Hunter, S. Chien, and J. Y.-J. Shyy, "Fluid Shear Stress Activation of Focal Adhesion Kinase: LINKING TO MITOGEN-ACTIVATED PROTEIN KINASES", *Journal of Biological Chemistry*, vol. 272, no. 48, pp. 30 455–30 462, Nov. 1997.

[34] T. E. Walshe, N. G. dela Paz, and P. A. D'Amore, "The Role of Shear-Induced Transforming Growth Factor-β Signaling in the Endothelium", *Arteriosclerosis, Thrombosis, and Vascular Biology*, vol. 33, no. 11, pp. 2608–2617, Nov. 2013.

[35] E. Mattila, K. Auvinen, M. Salmi, and J. Ivaska, "The protein tyrosine phosphatase TCPTP controls VEGFR2 signalling", *Journal of Cell Science*, vol. 121, no. 21, pp. 3570–3580, Nov. 2008.

[36] J. C. Kovacic, N. Mercader, M. Torres, M. Boehm, and V. Fuster, "Epithelial-to-mesenchymal and endothelial-to-mesenchymal transition: From cardiovascular development to disease", *Circulation*, vol. 125, no. 14, pp. 1795–1808, Apr. 2012.

[37] G. Bindea, B. Mlecnik, H. Hackl, P. Charoentong, M. Tosolini, A. Kirilovsky, W.-H. Fridman, F. Pagès, Z. Trajanoski, and J. Galon, "ClueGO: A Cytoscape plug-in to decipher functionally grouped gene ontology and pathway annotation networks", *Bioinformatics (Oxford, England)*, vol. 25, no. 8, pp. 1091–1093, Apr. 2009.

[38] H. Motulsky, *Intuitive biostatistics: a nonmathematical guide to statistical thinking*, Fourth edition. New York: Oxford University Press, 2018.

[39] G. García-Cardeña, K. R. Anderson, L. Mauri, and M. A. Gimbrone, "Distinct Mechanical Stimuli Differentially Regulate the PI3K/Akt Survival Pathway in Endothelial Cells", *Annals of the New York Academy of Sciences*, vol. 902, no. 1, pp. 294–297, Jan. 2006.

[40] M. Qin, Y. Luo, X.-b. Meng, M. Wang, H.-w. Wang, S.-y. Song, J.-x. Ye, R.-l. Pan, F. Yao, P. Wu, G.-b. Sun, and X.-b. Sun, "Myricitrin attenuates endothelial cell apoptosis to prevent atherosclerosis: An insight into PI3K/Akt activation and STAT3 signaling pathways", *Vascular Pharmacology*, vol. 70, pp. 23–34, Jul. 2015.

[41] G. Tie, J. Yan, Y. Yang, B. D. Park, J. A. Messina, R. L. Raffai, P. T. Nowicki, and L. M. Messina, "Oxidized Low-Density Lipoprotein Induces Apoptosis in Endothelial Progenitor Cells by Inactivating the Phosphoinositide 3-Kinase/Akt Pathway", *Journal of Vascular Research*, vol. 47, no. 6, pp. 519–530, 2010.

[42] S. Rosciglione, C. Thériault, M.-O. Boily, M. Paquette, and C. Lavoie, "Gαs regulates the post-endocytic sorting of G protein-coupled receptors", *Nature Communications*, vol. 5, no. 1, p. 4556, Dec. 2014.

[43] E. Galkina and K. Ley, "Vascular Adhesion Molecules in Atherosclerosis", *Arteriosclerosis, Thrombosis, and Vascular Biology*, vol. 27, no. 11, pp. 2292–2301, Nov. 2007.

[44] B. A. Hemmings and D. F. Restuccia, "PI3K-PKB/Akt pathway", *Cold Spring Harbor Perspectives in Biology*, vol. 4, no. 9, a011189, Sep. 2012.

[45] K. Tsoyi, H. J. Jang, I. T. Nizamutdinova, K. Park, Y. M. Kim, H. J. Kim, H. G. Seo, J. H. Lee, and K. C. Chang, "PTEN differentially regulates expressions of ICAM-1 and VCAM-1 through

PI3K/Akt/GSK-3β/GATA-6 signaling pathways in TNF-α-activated human endothelial cells", *Atherosclerosis*, vol. 213, no. 1, pp. 115–121, Nov. 2010.

[46] V Andres, "Control of vascular cell proliferation and migration by cyclin-dependent kinase signalling: New perspectives and therapeutic potential", *Cardiovascular Research*, vol. 63, no. 1, pp. 11–21, Jul. 2004.

[47] S. Akimoto, M. Mitsumata, T. Sasaguri, and Y. Yoshida, "Laminar Shear Stress Inhibits Vascular Endothelial Cell Proliferation by Inducing Cyclin-Dependent Kinase Inhibitor p21 $^{sdi1/cip1/waf1}$ ", *Circulation Research*, vol. 86, no. 2, pp. 185–190, Feb. 2000.

[48] D. J. Beech and A. C. Kalli, "Force Sensing by Piezo Channels in Cardiovascular Health and Disease", *Arteriosclerosis, Thrombosis, and Vascular Biology*, vol. 39, no. 11, pp. 2228–2239, Nov. 2019.

[49] A. H. Lewis, A. F. Cui, M. F. McDonald, and J. Grandl, "Transduction of Repetitive Mechanical Stimuli by Piezo1 and Piezo2 Ion Channels", *Cell Reports*, vol. 19, no. 12, pp. 2572–2585, Jun. 2017.

[50] H. Yang, C. Liu, R.-M. Zhou, J. Yao, X.-M. Li, Y. Shen, H. Cheng, J. Yuan, B. Yan, and Q. Jiang, "Piezo2 protein: A novel regulator of tumor angiogenesis and hyperpermeability", *Oncotarget*, vol. 7, no. 28, pp. 44 630–44 643, Jul. 2016.

[51] J. Guo, Z. Wang, J. Wu, M. Liu, M. Li, Y. Sun, W. Huang, Y. Li, Y. Zhang, W. Tang, X. Li, C. Zhang, F. Hong, N. Li, J. Nie, and F. Yi, "Endothelial SIRT6 Is Vital to Prevent Hypertension and Associated Cardiorenal Injury Through Targeting Nkx3.2-GATA5 Signaling", *Circulation Research*, vol. 124, no. 10, pp. 1448–1461, May 2019.

[52] F. Li, H. Qu, H.-C. Cao, M.-H. Li, C. Chen, X.-F. Chen, B. Yu, L. Yu, L.-M. Zheng, and W. Zhang, "Both FOXO3a and FOXO1 are involved in the HGF-protective pathway against apoptosis in endothelial cells: The function of FOXO3a and FOXO1 in endothelial cells", *Cell Biology International*, vol. 39, no. 10, pp. 1131–1137, Oct. 2015.

[53] H.-Y. Lee, H.-J. You, J.-Y. Won, S.-W. Youn, H.-J. Cho, K.-W. Park, W.-Y. Park, J.-S. Seo, Y.-B. Park, K. Walsh, B.-H. Oh, and H.-S. Kim, "Forkhead Factor, FOXO3a, Induces Apoptosis of Endothelial

Cells Through Activation of Matrix Metalloproteinases", *Arteriosclerosis, Thrombosis, and Vascular Biology*, vol. 28, no. 2, pp. 302–308, Feb. 2008.

[54] T. Czymai, D. Viemann, C. Sticht, G. Molema, M. Goebeler, and M. Schmidt, "FOXO3 Modulates Endothelial Gene Expression and Function by Classical and Alternative Mechanisms", *Journal of Biological Chemistry*, vol. 285, no. 14, pp. 10 163–10 178, Apr. 2010.

[55] H. Song, J.-i. Suehiro, Y. Kanki, Y. Kawai, K. Inoue, H. Daida, K. Yano, T. Ohhashi, P. Oettgen, W. C. Aird, T. Kodama, and T. Minami, "Critical Role for GATA3 in Mediating Tie2 Expression and Function in Large Vessel Endothelial Cells", *Journal of Biological Chemistry*, vol. 284, no. 42, pp. 29 109–29 124, Oct. 2009.

[56] M. Umetani, C. Mataki, N. Minegishi, M. Yamamoto, T. Hamakubo, and T. Kodama, "Function of GATA Transcription Factors in Induction of Endothelial Vascular Cell Adhesion Molecule-1 by Tumor Necrosis Factor-α", *Arteriosclerosis, Thrombosis, and Vascular Biology*, vol. 21, no. 6, pp. 917–922, Jun. 2001.

[57] N. Froese, B. Kattih, A. Breitbart, A. Grund, R. Geffers, J. D. Molkentin, A. Kispert, K. C. Wollert, H. Drexler, and J. Heineke, "GATA6 Promotes Angiogenic Function and Survival in Endothelial Cells by Suppression of Autocrine Transforming Growth Factor β/Activin Receptor-like Kinase 5 Signaling", *Journal of Biological Chemistry*, vol. 286, no. 7, pp. 5680–5690, Feb. 2011.

[58] G. Hu and K. Zhao, "Correlating Histone Modification Patterns with Gene Expression Data During Hematopoiesis", in *Stem Cell Transcriptional Networks*, B. L. Kidder, Ed., vol. 1150, Series Title: Methods in Molecular Biology, New York, NY: Springer New York, 2014, pp. 175–187.

[59] D. Chen, K. Walsh, and J. Wang, "Regulation of cdk2 Activity in Endothelial Cells That Are Inhibited From Growth by Cell Contact", *Arteriosclerosis, Thrombosis, and Vascular Biology*, vol. 20, no. 3, pp. 629–635, Mar. 2000.

[60] K.-C. Wang, Y.-T. Yeh, P. Nguyen, E. Limqueco, J. Lopez, S. Thorossian, K.-L. Guan, Y.-S. J. Li, and S. Chien, "Flow-dependent YAP/TAZ activities regulate endothelial phenotypes and atherosclerosis",

Proceedings of the National Academy of Sciences of the United States of America, vol. 113, no. 41, pp. 11 525–11 530, 2016.

[61] S. Xu, M. Koroleva, M. Yin, and Z. G. Jin, "Atheroprotective laminar flow inhibits Hippo pathway effector YAP in endothelial cells", *Translational Research*, vol. 176, 18–28.e2, Oct. 2016.

[62] D. Gong and J. E. Ferrell, "The roles of cyclin A2, B1, and B2 in early and late mitotic events", *Molecular Biology of the Cell*, vol. 21, no. 18, pp. 3149–3161, Sep. 2010.

[63] T. L. Marin, B. Gongol, F. Zhang, M. Martin, D. A. Johnson, H. Xiao, Y. Wang, S. Subramaniam, S. Chien, and J. Y.-J. Shyy, "AMPK promotes mitochondrial biogenesis and function by phosphorylating the epigenetic factors DNMT1, RBBP7, and HAT1", *Science Signaling*, vol. 10, no. 464, eaaf7478, Jan. 2017.

[64] T. Jain, E. A. Nikolopoulou, Q. Xu, and A. Qu, "Hypoxia inducible factor as a therapeutic target for atherosclerosis", *Pharmacology & Therapeutics*, vol. 183, pp. 22–33, Mar. 2018.

[65] N. Skuli, L. Liu, A. Runge, T. Wang, L. Yuan, S. Patel, L. Iruela-Arispe, M. C. Simon, and B. Keith, "Endothelial deletion of hypoxia-inducible factor-2alpha (HIF-2alpha) alters vascular function and tumor angiogenesis", *Blood*, vol. 114, no. 2, pp. 469–477, Jul. 2009.

[66] M. Molino, M. J. Woolkalis, N. Prevost, D. Praticó, E. S. Barnathan, G. Taraboletti, B. S. Haggarty, J. Hesselgesser, R. Horuk, J. A. Hoxie, and L. F. Brass, "CXCR4 on human endothelial cells can serve as both a mediator of biological responses and as a receptor for HIV-2", *Biochimica et Biophysica Acta (BBA) - Molecular Basis of Disease*, vol. 1500, no. 2, pp. 227–240, Feb. 2000.

[67] Y. Döring, H. Noels, E. P. C. van der Vorst, C. Neideck, V. Egea, M. Drechsler, M. Mandl, L. Pawig, Y. Jansen, K. Schröder, K. Bidzhekov, R. T. A. Megens, W. Theelen, B. M. Klinkhammer, P. Boor, L. Schurgers, R. van Gorp, C. Ries, P. J. H. Kusters, A. van der Wal, T. M. Hackeng, G. Gäbel, R. P. Brandes, O. Soehnlein, E. Lutgens, D. Vestweber, D. Teupser, L. M. Holdt, D. J. Rader, D. Saleheen, and C. Weber, "Vascular CXCR4 Limits Atherosclerosis by Maintaining Arterial Integrity: Evidence From Mouse and Human Studies", *Circulation*, vol. 136, no. 4, pp. 388–403, Jul. 2017.

[68] R. Melchionna, D. Porcelli, A. Mangoni, D. Carlini, G. Liuzzo, G. Spinetti, A. Antonini, M. C. Capogrossi, and M. Napolitano, "Laminar shear stress inhibits CXCR4 expression on endothelial cells: Functional consequences for atherogenesis", *The FASEB Journal*, vol. 19, no. 6, pp. 1–25, Apr. 2005.

[69] D. R. Sweet, L. Fan, P. N. Hsieh, and M. K. Jain, "Krüppel-Like Factors in Vascular Inflammation: Mechanistic Insights and Therapeutic Potential", *Frontiers in Cardiovascular Medicine*, vol. 5, p. 6, Feb. 2018.

[70] Y. Miao, N. E. Ajami, T.-S. Huang, F.-M. Lin, C.-H. Lou, Y.-T. Wang, S. Li, J. Kang, H. Munkacsi, M. R. Maurya, S. Gupta, S. Chien, S. Subramaniam, and Z. Chen, "Enhancer-associated long non-coding RNA LEENE regulates endothelial nitric oxide synthase and endothelial function", *Nature Communications*, vol. 9, no. 1, p. 292, Dec. 2018.

[71] X. Ma, P. Zhu, Y. Ding, H. Zhang, Q. Qiu, A. V. Dvornikov, Z. Wang, M. Kim, Y. Wang, M. Lowerison, Y. Yu, N. Norton, J. Herrmann, S. C. Ekker, T. K. Hsiai, X. Lin, and X. Xu, "Retinoid X receptor alpha is a spatiotemporally predominant therapeutic target for anthracycline-induced cardiotoxicity", *Science Advances*, vol. 6, no. 5, eaay2939, Jan. 2020.

[72] M. I. Cybulsky, K. Iiyama, H. Li, S. Zhu, M. Chen, M. Iiyama, V. Davis, J.-C. Gutierrez-Ramos, P. W. Connelly, and D. S. Milstone, "A major role for VCAM-1, but not ICAM-1, in early atherosclerosis", *Journal of Clinical Investigation*, vol. 107, no. 10, pp. 1255–1262, May 2001.

[73] C. Dong, W. Yoon, and P. J. Goldschmidt-Clermont, "DNA Methylation and Atherosclerosis", *The Journal of Nutrition*, vol. 132, no. 8, 2406S–2409S, Aug. 2002.

[74] S. Tabaei and S. S. Tabaee, "DNA methylation abnormalities in atherosclerosis", *Artificial Cells, Nanomedicine, and Biotechnology*, vol. 47, no. 1, pp. 2031–2041, Dec. 2019.

[75] B. Illi, S. Nanni, A. Scopece, A. Farsetti, P. Biglioli, M. C. Capogrossi, and C. Gaetano, "Shear Stress–Mediated Chromatin Remodeling Provides Molecular Basis for Flow-Dependent Regulation of Gene Expression", *Circulation Research*, vol. 93, no. 2, pp. 155–161, Jul. 2003.

[76] O. Bondareva, R. Tsaryk, V. Bojovic, M. Odenthal-Schnittler, A. F. Siekmann, and H.-J. Schnittler, "Identification of atheroprone shear stress responsive regulatory elements in endothelial cells", *Cardiovascular Research*, vol. 115, no. 10, pp. 1487–1499, Aug. 2019.

[77] A. Greißel, M. Culmes, R. Burgkart, A. Zimmermann, H.-H. Eckstein, A. Zernecke, and J. Pelisek, "Histone acetylation and methylation significantly change with severity of atherosclerosis in human carotid plaques", *Cardiovascular Pathology*, vol. 25, no. 2, pp. 79–86, Mar. 2016.

[78] J. L. Harman, L. Dobnikar, J. Chappell, B. G. Stokell, A. Dalby, K. Foote, A. Finigan, P. Freire-Pritchett, A. L. Taylor, M. D. Worssam, R. R. Madsen, E. Loche, A. Uryga, M. R. Bennett, and H. F. Jørgensen, "Epigenetic Regulation of Vascular Smooth Muscle Cells by Histone H3 Lysine 9 Dimethylation Attenuates Target Gene-Induction by Inflammatory Signaling", *Arteriosclerosis, Thrombosis, and Vascular Biology*, vol. 39, no. 11, pp. 2289–2302, Nov. 2019.

[79] M. He, T.-S. Huang, S. Li, H.-C. Hong, Z. Chen, M. Martin, X. Zhou, H.-Y. Huang, S.-H. Su, J. Zhang, W.-T. Wang, J. Kang, H.-D. Huang, J. Zhang, S. Chien, and J. Y.-J. Shyy, "Atheroprotective Flow Upregulates ITPR3 (Inositol 1,4,5-Trisphosphate Receptor 3) in Vascular Endothelium via KLF4 (Krüppel-Like Factor 4)-Mediated Histone Modifications", *Arteriosclerosis, Thrombosis, and Vascular Biology*, vol. 39, no. 5, pp. 902–914, May 2019.

[80] K. R. Karch, J. E. DeNizio, B. E. Black, and B. A. Garcia, "Identification and interrogation of combinatorial histone modifications", *Frontiers in Genetics*, vol. 4, 2013.

[81] A. Lindner, B. Charra, D. J. Sherrard, and B. H. Scribner, "Accelerated Atherosclerosis in Prolonged Maintenance Hemodialysis", *New England Journal of Medicine*, vol. 290, no. 13, pp. 697–701, Mar. 1974.

[82] J. M. Valdivielso, D. Rodríguez-Puyol, J. Pascual, C. Barrios, M. Bermúdez-López, M. D. Sánchez-Niño, M. Pérez-Fernández, and A. Ortiz, "Atherosclerosis in Chronic Kidney Disease: More, Less, or Just Different?", *Arteriosclerosis, Thrombosis, and Vascular Biology*, vol. 39, no. 10, pp. 1938–1966, Oct. 2019.